

HONG KONG

MEDICAL JOURNAL

香港醫學雜誌

The official publication of the
Hong Kong Academy of Medicine and
the Hong Kong Medical Association

26(57)

HONG KONG MEDICAL JOURNAL

香港醫學雜誌

Volume 26 Number 6 December 2020

Supplement 7

Health and Medical Research Fund

Research Dissemination Reports

醫療衛生研究基金

研究成果報告

Children's health
兒童健康

Neurology
神經病學

Stroke / brain injury
中風/腦損傷



ISSN 1024-2708

香港醫學專科學院出版社
HONG KONG ACADEMY OF MEDICINE PRESS

MEDICAL JOURNAL

香港醫學雜誌

EDITOR-IN-CHIEF

Martin CS Wong 黃全生

SENIOR EDITORS

LW Chu 朱亮榮

Albert KK Chui 徐家強

Michael G Irwin

Eric CH Lai 賴俊雄

KY Leung 梁國賢

Anthony CF Ng 吳志輝

TW Wong 黃大偉

EDITORS

KS Chan 陳健生

Sherry KW Chan 陳詒輝

Jason PY Cheung 鍾培言

Kelvin KL Chong 莊金隆

Velda LY Chow 周令宇

Jacqueline PW Chung 鍾佩樺

James TK Fung 馮德焜

Brian SH Ho 何思灝

Ellis KL Hon 韓錦倫

Junjie Huang 黃傑文

KW Huang 黃凱文

WK Hung 熊維嘉

Bonnie CH Kwan 關清霞

Ho Lam 林贊賢

Arthur CW Lau 劉俊穎

PY Lau 婁培友

Danny WH Lee 李偉雄

Thomas WH Leung 梁慧康

WK Leung 梁惠強

Kenneth KW Li 李啟煌

Janice YC Lo 羅懿之

Herbert HF Loong 龍浩鋒

Rashid Lui 雷諾信

James KH Luk 陸嘉熙

Arthur DP Mak 麥敦平

Henry KF Mak 麥嘉豐

Martin W Pak 白威基

Walter WK Seto 司徒偉珊

Regina WS Sit 薛詠珊

William YM Tang 鄧旭明

Jeremy YC Teoh 張源津

KY Tse 謝嘉瑜

Harry HX Wang 王皓翔

HL Wong 黃學良

Kenneth KY Wong 黃格元

Patrick CY Woo 胡釗逸

Hao Xue 薛浩

Jason CS Yam 任卓昇

Bryan PY Yan 甄秉言

TK Yau 游子覺

Kelvin KH Yiu 姚啟恒

Vivian MY Yuen 袁文英

EPIDEMIOLOGY ADVISERS

Daniel SY Ho 何世賢

Eman Leung 梁以文

Edmond SK Ma 馬紹強

Gary Tse 謝家偉

Shelly LA Tse 謝立亞

Ian YH Wong 王逸軒

Esther YT Yu 余懿德

Hunter KL Yuen 袁國禮

STATISTICAL ADVISERS

Marc KC Chong 莊家俊

William B Goggins

Eddy KF Lam 林國輝

Carlos KH Wong 黃競浩

HONORARY ADVISERS

David VK Chao 周偉強

Paul BS Lai 賴寶山

Health and Medical Research Fund**Research Dissemination Reports****Editorial**

3

CHILDREN'S HEALTH**Whole exome sequencing for developmental delay and learning difficulties: abridged secondary publication**

4

*SLJ Kwok, WLE Hau, TF Chan, FMI Lo, LWE Fung, SKW Tsui***Peak oxygen uptake in healthy Chinese children and adolescents by age, sex, and maturation**

7

*AM Li, A McManus, RYT Sung***MicroRNA and its link to osteoblasts in adolescent idiopathic scoliosis: abridged secondary publication**

10

*JCY Cheng, A Moreau, WYW Lee, TP Lam, BHK Yip, RKW Choy***NEUROLOGY****Home-based exercise intervention for caregivers of persons with dementia: a randomised controlled trial: abridged secondary publication**

13

*WC Chan, LCW Lam, N Lautenschlager, B Dow, SL Ma***Nanoparticles to identify Alzheimer disease by magnetic resonance imaging: abridged secondary publication**

17

*L Baum, AHL Chow, YX Wang, EX Wu, RG Pautler***Targeted drug discovery for Alzheimer disease: abridged secondary publication**

20

*AML Chan, L Baum, RCC Chang, JA Esteban, ZX Lin, YH Wong, WH Yung***Stochastic stimulation of the motor cortex for treating parkinsonian symptoms: abridged secondary publication**

23

*WH Yung, VCT Mok, YKe***Neuroprotective effects of oxyresveratrol on 6-hydroxydopamine on medial forebrain bundles in a rat model of Parkinson disease: abridged secondary publication**

26

*A Shah, YS Ho, KM Ng, M Wang, C Legido-Quigley, RCC Chang***Small molecule of adiponectin receptor agonist—AdipoRon—for Alzheimer disease: abridged secondary publication**

29

*RCL Ng, M Jian, M Bunting, SK Chung, KH Chan***Modified Huang-Lian-Jie-Du-Tang and its combination with memantine for Alzheimer disease: an in vivo study (abridged secondary publication)**

33

SSK Durairajan, M Li, SK Chung, QB Han, A Iyaswamy, SG Sreenivasamurthy, S Malampati, AK Kammala

**INTERNATIONAL EDITORIAL
ADVISORY BOARD**

Sabaratnam Arulkumaran
United Kingdom
Robert Atkins
Australia
Peter Cameron
Australia
Daniel KY Chan
Australia
David Christiani
United States
Andrew Coats
Australia
James Dickinson
Canada
Willard Fee, Jr
United States
Robert Hoffman
United States
Roger Jones
United Kingdom
Michael Kidd
Australia
Arthur Kleinman
United States
Stephen Leeder
Australia
Xiaoping Luo
PR China
William Rawlinson
Australia
Jonathan Samet
United States
Yaojiang Shi
PR China
David Weller
United Kingdom
Max Wintermark
United States
Wanghong Xu
PR China
Atsuyuki Yamataka
Japan
Homer Yang
Canada
KG Yeoh
Singapore
Matthew Yung
United Kingdom
Zhijie Zheng
PR China

Full details of the Editorial Board
are available online at
<https://www.hkmj.org/about/eo.html>

STROKE / BRAIN INJURY

Lutein for alleviating early high mortality and brain pathology after experimental stroke in a genetic type I diabetic mouse model: abridged secondary publication	37
<i>AKW Lai, DTC Ng, BKC Tam, FKC Fung, SK Chung, ACY Lo</i>	
Intracranial artery calcification to screen patients at high risk of recurrent stroke: abridged secondary publication	42
<i>KS Wong, XY Chen, TWH Leung, YW Siu, L Xiong, X Leng</i>	
Gastrodia-Uncaria water extract and tissue plasminogen activator for treating embolus-induced cerebral ischaemia: abridged secondary publication	45
<i>JW Xian, AYT Choi, WN Leung, L Li, CBS Lau, TWH Leung, CW Chan</i>	
Author index & Disclaimer	48

MANAGING EDITOR

Alan Purvis

DEPUTY MANAGING EDITOR

Betty Lau 劉薇薇

ASSISTANT MANAGING EDITOR

Warren Chan 陳俊華

Editorial

Dissemination reports are concise informative reports of health-related research supported by the Health and Medical Research Fund (and its predecessor funds) administered by the Food and Health Bureau. In this edition, we present 13 dissemination reports of projects related to children's health, neurology, and stroke and brain injury. In particular, three projects are highlighted due to their potentially significant findings, impact on healthcare delivery and practice, and/or contribution to health policy formulation in Hong Kong.

Developmental delay and learning difficulties originate mainly during embryogenesis or early brain development. Its prevalence in Hong Kong is about 1%. Whole-exome sequencing (WES) is a potentially valuable technique for diagnosing previously undiagnosed developmental disorders. Kwok et al¹ aimed to find the causative, small, single-nucleotide or multi-nucleotide mutations fitting monogenic dominant disease models and recessive disease models among 30 patient-parent trios of children with undiagnosed developmental delay. They found that WES is a cost-effective method for management of patients with apparently undiagnosed developmental delay or learning difficulties.

In Hong Kong, about 10% of older persons have dementia. Informal caregivers who provide the bulk of dementia care experience considerable stress. Caregivers are at an elevated risk of developing depression and anxiety and have poorer quality of life and perceived health, higher risk of hypertension, lower immunity, and elevated risk of mortality. Chan et al² compared the efficacy of a 12-step sitting Tai Chi home-based structured exercise programme

with a non-exercise social contact control group in the treatment for depression in both carers and care recipients. They found that the exercise programme alleviated mild depressive symptoms among caregivers. Both caregivers and care recipients had improved balance ability. The sitting Tai Chi programme offers a low-cost and safe treatment option for caregivers with mild depressive symptoms.

The incidence of stroke in patients with type 1 diabetes is about four-fold higher than in the general population. These patients tend to die from stroke, with shortened median survival and more haemorrhagic transformation. Lutein is an anti-inflammatory and anti-oxidative agent that has neuroprotective effects in wildtype mice upon middle cerebral artery occlusion. Lai et al³ aimed to identify the cause of exacerbation of symptoms in patients with diabetes upon stroke using a mouse model of type 1 diabetes and to determine the efficacy of lutein under hyperglycaemic conditions. It was found that lutein treatment was able to lower mortality (after long ischaemia) and neurological deficits (after short ischaemia). Lutein is therefore a potential treatment for stroke patients with type 1 diabetes. Further studies are required before clinical application.

We hope you will enjoy this selection of research dissemination reports. Electronic copies of these dissemination reports and the corresponding full reports can be downloaded individually from the Research Fund Secretariat website (<https://rfs2.fhb.gov.hk/>). Researchers interested in the funds administered by the Food and Health Bureau also may visit the website for detailed information about application procedures.

Supplement co-editors



Dr Richard A Collins
Chief Scientific Reviewer
(Research Office)
Food and Health Bureau



Dr Martin Chan Chi-wai
Senior Scientific Reviewer
(Research Office)
Food and Health Bureau

References

1. Kwok SLJ, Hau WLE, Chan TF, Lo FMI, Fung LWE, Tsui SKW. Whole exome sequencing for developmental delay and learning difficulties: abridged secondary publication. *Hong Kong Med J* 2020;26(Suppl 7):S4-6.
2. Chan WC, Lam LCW, Lautenschlager N, Dow B, Ma SL. Home-based exercise intervention for caregivers of persons with dementia: a randomised controlled trial: abridged secondary publication. *Hong Kong Med J* 2020;26(Suppl 7):S13-6.
3. Lai AKW, Ng DTC, Tam BKC, Fung FKC, Chung SK, Lo ACY. Lutein for alleviating early high mortality and brain pathology after experimental stroke in a genetic type I diabetic mouse model: abridged secondary publication. *Hong Kong Med J* 2020;26(Suppl 7):S37-41.

Whole exome sequencing for developmental delay and learning difficulties: abridged secondary publication

SLJ Kwok, WLE Hau, TF Chan, FMI Lo, LWE Fung, SKW Tsui *

KEY MESSAGES

1. Whole exome sequencing (WES) was performed for 30 patient-parent trios of children with undiagnosed developmental delay.
2. Our bioinformatics pipeline coupled with clinical review confirmed the diagnosis by *de novo* mutations or inherited compound heterozygous rare variants in seven (24%) patients. In addition, possible causative variants were found in three other patients.
3. WES is a cost-efficient method for management of patients with apparently undiagnosed developmental delay or learning difficulties after first-tier testing.

Hong Kong Med J 2020;26(Suppl 7):S4-6

HMRP project number: 01120596

¹ SLJ Kwok, ² WLE Hau, ^{3,4} TF Chan, ² FMI Lo, ⁵ LWE Fung, ^{1,4} SKW Tsui

¹ School of Biomedical Sciences, The Chinese University of Hong Kong, Hong Kong

² Clinical Genetic Service, Department of Health, Hong Kong

³ School of Life Sciences, The Chinese University of Hong Kong, Hong Kong

⁴ Hong Kong Bioinformatics Centre, The Chinese University of Hong Kong, Hong Kong

⁵ Department of Paediatrics, The Chinese University of Hong Kong, Hong Kong

* Principal applicant and corresponding author: kwtsui@cuhk.edu.hk

Introduction

Developmental disorder (DD) encompasses developmental delay and learning difficulties. It is a disorder in which the most prominent pathogenetic mechanism occurs during embryogenesis or early brain development.¹ In Hong Kong, the total number of persons with intellectual disability was estimated to be 71 000 to 101 000, representing a prevalence of 1.0% to 1.4%. First-tier tests such as G-banding karyotyping and array chromosome genomic hybridisation have low diagnostic yield. Recently, whole-exome sequencing (WES) has been successful in diagnosing 30% of previously undiagnosed DDs.² We aim to find the causative, small, single-nucleotide or multi-nucleotide mutations fitting monogenic dominant disease models (such as *de novo* mutations [DNMs]) and recessive disease models.

Methods

Patients with undiagnosed DDs and their parents were recruited through Prince of Wales Hospital, The Chinese University of Hong Kong, and Clinical Genetic Service of the Department of Health in Hong Kong. They had negative results of first-tier tests (G-banding karyotyping and array chromosome genomic hybridisation). Those with potentially acquired causes to explain their DDs were excluded. Informed written consent was obtained from both parents for all patients who were under 18 years old. Clinical data of initial apparent phenotypes were collected. Peripheral blood was collected from each patient-parent trio. QIAamp DNA Blood Mini kit

(Qiagen) was used to extract genomic DNA (gDNA) according to the manufacturer's protocol. The purified, quality-passed samples were sent to Beijing Genomics Institute for sequencing.

WES data were preprocessed according to the GATK Best Practices version 3. For the variant prioritisation, GEMINI was chosen as the SQL-based interface to first query the variants according to various inheritance patterns including *de novo* 'inheritance'. GEMINI requires Vt to preprocess the files. Vt was also used to decompose and normalise variants. The resulting normalised VCF file underwent functional annotation using the Ensembl Variant Effect Predictor version 84, with the option enabled for PolyPhen and SIFT predictions of deleteriousness of missense variants.

The annotated VCF file was then loaded into a SQL database using the GEMINI 'load' command. To find DNMs, the GEMINI '*de novo*' command was used. The number of DNMs per human exome is usually <5 and therefore no filtering criteria (eg, functional deleteriousness prediction) were applied. Besides, we were interested in any type of DNM in or flanking the exons. To find the variants fitting the compound heterozygous or autosomal homozygous recessive inheritance models, the GEMINI commands 'comp_hets' and 'autosomal_recessive' were used. For X-linked hemizygous variants, the GEMINI 'query' command was used, which allows one to construct flexible genotype queries that can be set to filter for said variants. For the final step of variant prioritisation via bioinformatics pipeline, we wrote a custom script in Perl to automatically

indicate whether a gene in the GEMINI query output matched a known DD gene according to the Developmental Disorders Genotype-to-Phenotype database, as well as the reported allelic requirement for the DD to manifest (ie, dominant/monoallelic or recessive/biallelic). The shortlisted variants per patient were then handed over to the clinicians of our team, who then reviewed previous case reports of DD patients with the same gene with clinically and/or experimentally confirmed causative mutation.

Results

A total of 30 patients with undiagnosed DDs and their parents were recruited. After basic quality filtering by VQSR and depth, the bottom approximately 30% of worst-quality or low-depth variants were removed. The Table shows patients with clinically confirmed and validated DNMs or compound heterozygous variants.

Patient 4 with SCN8A DNM was deemed causative. Her clinician prescribed sodium channel blocker (Trileptal) to improve her seizures but her seizures got worse again a few months later. The clinician also performed vagal nerve stimulation in December 2015, and the patient's condition appeared to stabilise.

Patient 28 with another SCN8A DNM had a relatively stable condition. The clinician did not change prescription after diagnosis, because the family requested so.

Patient 10 had CACNA1A DNM, which the clinician attributed to his chronic ataxia and recurrent hemiparesis. At least six mutations in this

gene were reported to be associated with familial hemiplegic migraine and cerebellar signs, including T666M, R583Q, D715E, Y1385C, R1668W, and W1684R.³ These can be explained by high expression of $\alpha 1$ subunit in the cerebellum, involving the Purkinje and granules cells.

Patient 14 was referred for delayed development with DNM in GRIN2B. There are studies supporting the contribution of GRIN2B to developmental issues and autistic features in children. Specifically, the stereotypical hand movement, which was a form of behavioural phenotype noticed in our patient, was delineated with the GRIN2B mutation.

In patient 16, the mutated GNAO1 gene is abundant in brain tissue and is believed to be important in brain function. Although patient 16 did not present with epilepsy, the clinical features of DD and involuntary movement could be explained with GNAO1 DNM.

Patient 20 has an X-linked ATRX variant inherited from his mother. His blood was taken for further non-genetic investigation. His clinical features were compatible with the diagnosis of X-linked alpha thalassemia mental retardation.

Patient 23 had multiple problems (in addition to learning difficulties) throughout years of follow-up in the Clinical Genetic Service. She had a progressive loss of vision, obesity, short stature, increased serum lipid level with fatty liver, and mild thyroid dysfunction. All these features were compatible with the diagnosis of Alstrom syndrome, which was causally related to ALMS1 mutations. The ALMS1 compound heterozygous frameshift

TABLE. Patients with clinically confirmed mutations

Patient of trio	Gene	Mutation inheritance type	mRNA mutation in HGVS notation	Protein mutation in HGVS notation	Mutation consequence type	Deleterious prediction by programs (damaging or neutral)				
						CADD	SIFT	Pol-Phen-2	PRO-VEAN	FATHMM
4	SCN8A	DNM	NM_014191.3:c.4862T>G	NP_055006.1:p.Leu1621Trp	Missense	Damaging	Damaging	Damaging	Damaging	Damaging
7	POLR1C	Compound heterozygous	NM_203290.3:c.436T>C	NP_976035.1:p.Cys146Arg	Missense	Damaging	Damaging	Damaging	Damaging	Damaging
	POLR1C	Compound heterozygous	NM_203290.3:c.883_885delAAG	NP_976035.1:p.Lys295del	In-frame deletion	Damaging	N/A	N/A	Damaging	N/A
10	CACNA1A	DNM	NM_000834.3:c.2065G>A	NP_000825.2:p.Gly689Ser	Missense	Damaging	Damaging	Damaging	Damaging	Damaging
14	GRIN2B	DNM	NM_000834.3:c.2065G>A	NP_000825.2:p.Gly689Ser	Missense	Damaging	Damaging	Damaging	Damaging	Neutral
16	GNAO1	DNM	NM_020988.2:c.736G>A	NP_066268.1:p.Gly246Lys	Missense	Damaging	Damaging	Damaging	Damaging	Damaging
20	ATRX	X-linked	ENST00000373344.5:c.536A>G	ENSP00000362441.4:p.Asn179Ser	Missense	Damaging	Damaging	Damaging	Damaging	Damaging
23	ALMS1	Compound heterozygous	ENST00000264448.6:c.4911_4914delTAAA	ENSP00000264448.6:p.Asn1637LysfsTer4	Frameshift	Damaging	N/A	N/A	N/A	N/A
	ALMS1	Compound heterozygous	ENST00000264448.6:c.11110_11128delAGGTCTAATCAAATTAATAA	ENSP00000264448.6:p.Arg3704LeufsTer11	Frameshift	Damaging	N/A	N/A	N/A	N/A
24	PPP2R5D	DNM	NM_006245.3:c.592G>A	NP_006236.1:p.Glu198Lys	Missense	Damaging	Damaging	Damaging	Damaging	Neutral
26	MAGEL2	DNM	NM_019066.4:c.187dupC	NP_061939.3:p.Gln63ProfsTer47	Frameshift	Damaging	N/A	N/A	N/A	N/A
28	SCN8A	DNM	NM_014191.3:c.434A>G	Np_055006.1:p.Asn145Ser	Missense	Damaging	Damaging	Damaging	Damaging	Damaging

mutations identified could fully support a valid genotype-phenotype correlation.

Patient 13 had congenital heart disease and poor muscle tone. The DNM found in TRRAP (transformation/transcription domain-associated protein), which is the cofactor of the histone acetyltransferase, might play a role in controlling cell-cycle progression and neurogenesis.

Patient 15 had moderate learning difficulties, extra digit, hydrocephalus, and dysmorphic facial features. These features might be related to the PRPF8 DNM. Individuals with this mutation may have various problems because PRPF8 gene variant was found to link to the regulatory potential of altering the core spliceosome machinery.

Patient 26 was clinically suspected to have Prader-Willi syndrome because of severe learning difficulties, marked hypotonia, small head, and relevant facial characteristics. Although MAGEL2 DNM is related to Prader-Willi syndrome, the truncating mutation in our patient differed from it.

Discussion

WES of patient-parent trios enables mutation calling according to inheritance patterns. Parents can act as healthy controls (at least clinically healthy although there is a possibility of subclinical symptoms of DD) and provide the best genetic background controls.

After basic quality filtering by VQSR and depth, the bottom 30% of worst-quality or low-depth variants were removed. This helped prioritise variants. For example, a DNM is a type of Mendelian violation, and therefore a considerable portion of the worst-quality variants are Mendelian violations. Basic variant filtering helps reduce the time spent on manually excluding false positives. Also, a lot of low-quality genotype variants are false positives and filtered out. False positives should be minimised during the bioinformatics analysis when possible. However, most filtering recommendations are conservative in order to avoid excluding true positive variants that might be of clinical significance.

In this study, the pipeline we developed is sufficient to make clinical diagnosis, with a success rate similar to previous small- and medium-scale exome studies. Recently, the ExAC consortium pointed out that many exome studies had been over-conservative in prioritising variants, especially on over-emphasising rare variants, leaving many potentially DD causative variants to be filtered out.⁴ In another study of protein-coding genes that were almost depleted of loss-of-function variants, 70% of the genes were not associated with DDs.⁵

In our earlier pipeline, if the clinician deemed the DNM as not causative, then we looked for recessive variants. Later, we modified the pipeline so that the preliminarily prioritised variants of all

inheritance types (ie, compound heterozygous, autosomal recessive, X-linked hemizygous) were queried together and collectively sent to the clinicians. Preliminary prioritisation by the research staff was appropriate because the clinicians only need to confirm variants with previous case reports.

For the clinical management, patient 4 was given new drug and palliative treatment according to his SCN8A DNM diagnosis. The discovery of CACNA1A DNM in patient 10 corrected the diagnosis of hemiplegic migraine. The diagnosis of patient 20 helped the clinician decide on follow-up after confirming already available clinical features. Other diagnosed patients mostly used the WES results for genetic counselling.

Conclusion

Making a genetic diagnosis for DD can avoid unnecessary investigations and enable the use of potentially more useful drugs (eg, sodium channel blocker), early consideration of palliative surgery (eg, vagal nerve stimulation), counselling on the risk of sudden unexpected death in epilepsy, and appropriate genetic counselling.

Funding

This study was supported by the Health and Medical Research Fund, Food and Health Bureau, Hong Kong SAR Government (#01120596). The full report is available from the Health and Medical Research Fund website (<https://rfs1.fhb.gov.hk/index.html>).

Disclosure

Part of the results of this research have been previously published in:

1. Fung LW, Kwok SL, Tsui KW. SCN8A mutations in Chinese children with early onset epilepsy and intellectual disability. *Epilepsia* 2015;56:1319-20.

References

1. Firth HV, Richards SM, Bevan AP, et al. DECIPHER: database of chromosomal imbalance and phenotype in humans using Ensembl resources. *Am J Hum Genet* 2009;84:524-33.
2. Deciphering Developmental Disorders Study. Large-scale discovery of novel genetic causes of developmental disorders. *Nature* 2015;519:223-8.
3. Ducros A, Denier C, Joutel A, et al. The clinical spectrum of familial hemiplegic migraine associated with mutations in a neuronal calcium channel. *N Eng J Med* 2001;345:17-24.
4. Lek M, Karczewski KJ, Minikel EV, et al. Analysis of protein-coding genetic variation in 60,706 humans. *Nature* 2016;536:285-91.
5. Walsh R, Thomson KL, Ware JS, et al. Reassessment of Mendelian gene pathogenicity using 7,855 cardiomyopathy cases and 60,706 reference samples. *Genet Med* 2017;19:192-203.

Peak oxygen uptake in healthy Chinese children and adolescents by age, sex, and maturation: abridged secondary publication

AM Li ^{*}, A McManus, RYT Sung

KEY MESSAGES

1. There are developmentally divergent trajectories for peak oxygen uptake between Southern Chinese and Caucasian children and adolescents.
2. When body mass is appropriately accounted for, peak oxygen uptake is greater in boys than girls from age 13 years, increasing with age in males but not in females.
3. Population-specific references are important for proper interpretation of cardiopulmonary exercise test parameters.

Hong Kong Med J 2020;26(Suppl 7):S7-9

HMRP project number: 02130486

¹ AM Li, ² A McManus, ¹ RYT Sung

¹ Department of Paediatrics, Prince of Wales Hospital, The Chinese University of Hong Kong, Hong Kong

² School of Health and Exercise Sciences, The University of British Columbia, Canada

* Principal applicant and corresponding author: albertmli@cuhk.edu.hk

Introduction

Peak oxygen uptake (VO_2) is defined as the greatest oxygen uptake elicited in a maximal exercise test and is considered the best indicator of cardiopulmonary fitness. We aimed to develop peak VO_2 references by age, sex, and maturation for Hong Kong Chinese children and adolescents aged 8 to 16 years.

Methods

The study protocol was approved by the Joint Chinese University of Hong Kong – New Territories East Clinical Research Ethics Committee. Chinese children and adolescents aged 8 to 16 years were recruited from randomly selected primary and secondary schools from four geographical regions of Hong Kong. Those with acute or chronic illness or recent upper respiratory tract or other infection within the past 4 weeks were excluded. Participants were assessed at the cardiopulmonary exercise laboratory in the Prince of Wales Hospital.

Body weight and percentage body fat were measured using foot-to-foot bioelectrical impedance (TBF-401, Tanita, Tokyo, Japan). Height was measured to the nearest 0.5 cm with a Harpenden stadiometer (Holtain, Grymych, UK).¹ Participants were asked to choose the most appropriate stage that best indicated their own sexual maturity using the Tanner pubertal self-assessment questionnaire.

Cardiopulmonary fitness was assessed using a maximal treadmill running test.² Heart rate was monitored. Breath-by-breath gas samples were collected using a comfortably fitted facemask and analysed using the Medgraphics System CPX/DTM

metabolic cart (Medical Graphics Corporation, St. Paul [MN], USA). Peak VO_2 was determined with standardised criteria.¹ Peak VO_2 ($\text{L}\cdot\text{min}^{-1}$) was ratio-scaled to body mass ($\text{mL}\cdot\text{kg}^{-1}\cdot\text{min}^{-1}$), fat-free mass ($\text{mL}\cdot\text{kg FFM}^{-1}\cdot\text{min}^{-1}$), and adjusted for body mass using an allometric model.

Participants were grouped according to age, sex, and maturation. Student's *t* test, Mann-Whitney *U* test, and Chi-square test were used for group comparisons for parametric, nonparametric, and categorical data, respectively. Group differences in peak VO_2 were compared using analysis of variance. The level of significance was set at 5%.

Percentile curves for log-linear-adjusted peak VO_2 (expressed in $\text{L}\cdot\text{min}^{-1}$) were constructed using the LMS method. The LMS method using the maximum penalised likelihood has been used to perform model fitting of the anthropometric centiles for the physical parameters.³

Results

Data from 852 children and adolescents aged 8 to 16 years were included in the final analyses (Table). Univariate analysis of variance showed that absolute peak VO_2 ($\text{L}\cdot\text{min}^{-1}$) differed by age ($P<0.001$), with a significant interaction ($P<0.001$). Follow-up analyses demonstrated an increase in absolute peak VO_2 ($\text{L}\cdot\text{min}^{-1}$) with age in both sexes. Pairwise comparisons confirmed that the difference in peak VO_2 ($\text{L}\cdot\text{min}^{-1}$) between boys and girls became apparent starting from age 12 years. When peak VO_2 was expressed as a ratio with body mass ($\text{mL}\cdot\text{kg}^{-1}\cdot\text{min}^{-1}$), similar results were observed, with significant main effects for age ($P<0.001$) and sex ($P<0.001$) and a significant

TABLE. Descriptive characteristic of the children

Characteristic	Boys (n=410)*	Girls (n=442)*	P value
Age, y	12.5±2.4	12.5±2.4	>0.05
Height, cm	153.5±15.4	150.4±11.3	<0.001
Weight, kg	46.1±14.1	42.6±11.7	<0.001
Body mass index, kg/m ²	19.2±3.7	18.5±3.3	0.004
Body fat, %	18.8±7.9 (n=289)	21.0±7.6 (n=300)	0.001
Fat free mass, kg	37.3±11.0 (n=289)	32.7±6.9 (n=300)	<0.001
Resting heart rate	82±14	85±14	0.001
Peak heart rate	196±10	195±9	0.241
Peak oxygen uptake (L·min ⁻¹)	2.00±0.73	1.58±0.44	<0.001
Predicted peak oxygen uptake (L·min ⁻¹)†	2.26±0.56	1.80±0.29	<0.001
Fat free mass-adjusted peak oxygen uptake (mL·kg ⁻¹ ·min ⁻¹)	56.1±8.4 (n=289)	51.3±6.8 (n=300)	<0.001
Peak oxygen uptake (mL·kg ⁻¹ ·min ⁻¹)	43.4±8.4	37.8±6.7	<0.001
RERmax	1.12±0.08	1.09±0.09	<0.001

* Data are presented as mean ± standard deviation

† Based on regression equations²: peak VO₂ for boys = -0.623+0.230 × age; peak VO₂ for girls = 0.253+0.124 × age

interaction (P<0.001). Peak VO₂ (mL·kg⁻¹·min⁻¹) increased with age in boys but remained relatively stable or slightly decreased in girls after age 10 years. Peak VO₂ (mL·kg⁻¹·min⁻¹) became significant different between boys and girls from age 12 years onwards (P<0.001). When peak VO₂ values were compared using an allometric model, there was sex difference in adjusted peak VO₂ (mL·kg⁻¹·min^{-0.77}) from age 13 years. Allometrically adjusted peak VO₂ increased with age in the boys only (P<0.001). There was no

significant main effect for age in girls.

Regarding the development of peak VO₂ by maturational status, univariate analysis of variance showed that absolute peak VO₂ (L·min⁻¹) differed by Tanner stage (P<0.001) and sex (P<0.001), with a significant interaction (P<0.001). Boys had a significantly higher absolute peak VO₂ (L·min⁻¹) than girls within each Tanner stage. These differences were greatest in Tanner stages IV and V. When peak VO₂ was scaled allometrically to body mass (mL·kg⁻¹·min^{-0.77}), there were significant main effects for Tanner stage (P<0.001) and sex (P<0.001), with a significant interaction (P<0.001). Pairwise comparisons confirmed that the difference in peak VO₂ (mL·kg⁻¹·min^{-0.77}) between sexes was apparent from Tanner stage 2 onwards. The allometrically adjusted peak VO₂ increased significantly with maturational in boys from Tanner stage 4 (P<0.001) only. In girls, there was a decline in allometrically scaled peak VO₂ at Tanner stage 3, but no differences between Tanner stages 1 and 2 and between Tanner stages 4 and 5 (P>0.05).

Using the LMS method, percentile curves for absolute peak VO₂ were constructed for boys and girls (Fig.).

Discussion

To the best of our knowledge, this is the only adequately powered study of treadmill-derived peak VO₂ of Hong Kong Chinese children and adolescents. Absolute peak VO₂ increased with age in both sexes, which is in accord with reports from elsewhere. When using an allometric model to account for differences in body mass, the adjusted peak VO₂ values from age 8 to 16 years were similar to previous work in Hong Kong Chinese boys⁴ and Caucasian

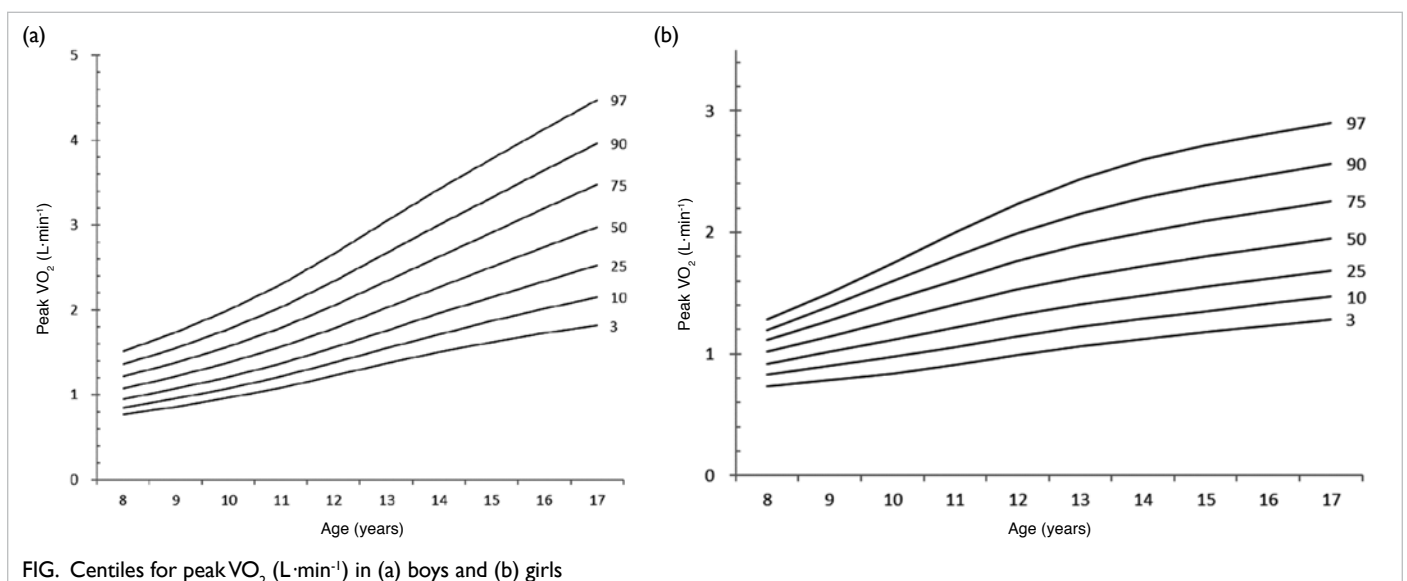


FIG. Centiles for peak VO₂ (L·min⁻¹) in (a) boys and (b) girls

boys, with a rise from age 13 years onwards. For girls, there was little variation in adjusted peak VO_2 across age. This is quite different from the pattern reported in Caucasian girls, who show a rise in peak VO_2 in early puberty, followed by a plateau.

Similar to previous studies, absolute peak VO_2 values were lower in girls than in boys. The difference in absolute and body mass-related peak VO_2 between boys and girls became significant from age 12 years, with the difference gradually widened as age increased. When an allometric model was applied, sex difference existed in adjusted peak VO_2 from age 13 years.

Compared to the predicted peak VO_2 ,⁵ the absolute peak VO_2 values from our Hong Kong children are considerably lower than those for Caucasian children. It is possible that Southern Chinese children reach peak height velocity at an earlier age, and this results in less time available for prepubertal growth and developmentally divergent peak VO_2 , compared with Caucasian children. Conventionally, peak VO_2 is expressed as a ratio standard with body mass. The developmental pattern of body mass-adjusted peak VO_2 declining with age in Hong Kong girls was similar to Caucasian girls and Northern Chinese girls. However, a different developmental pattern of body mass-adjusted peak VO_2 was observed in Hong Kong boys, with values remaining steady from age 8 to 12 years and gradually increased afterwards. This differs from observations in Northern Chinese boys that body mass-adjusted peak VO_2 increases from age 10 to 13 years and then remains steady. The theoretical and statistical limitations of the ratio standard to remove the effects of body mass have long been recognised. The use of allometric scaling removes the effects of body size and provides a better understanding of the actual developmental trajectory of peak VO_2 . We confirmed that allometrically scaled peak VO_2 in girls did not decline with age.

We calculated reference values for absolute peak VO_2 using the LMS method for different age groups in boys and girls. The LMS method has been used for constructing similar centile curves in paediatric growth charts and reference ranges. These centile curves provide population-specific references for proper interpretation of peak VO_2 in Hong Kong Chinese children and adolescents.

Conclusion

There are developmentally divergent trajectories for peak VO_2 in Southern Chinese children and adolescents, compared with Caucasian children. When body mass is appropriately accounted for, peak VO_2 is greater in boys than girls from age 13 years,

increasing with age in males but not in females. Moderate-to-vigorous physical activity is not related to allometrically scaled peak VO_2 . With adjustment by fat free mass, peak VO_2 is not impaired in students who are centrally obese.

Acknowledgements

We would like to thank Prof Yuen Man Pan Patrick and the Hong Kong Paediatric Bone Marrow Transplant Fund Research Grant for supporting the testing facilities of this project. We are most grateful to Dr Yu Chung Wah Clare for her technical support in performing the cardiopulmonary exercise test and for logistics arrangements, data processing, and report generation, Dr So Hung Kwan and Mr Au Chun Ting for their assistance in statistical analysis, Mr Tsang Fan Pong, Miss Tse Cheuk Wun Gogo, Miss Wong Tse Yan Lina, Miss Mak Ting Kun Grace, Miss Lau Hiu Yan Jubie, Miss Fong Oi Ling Hanna, and other helpers for their assistance in data collection. We would like to express our gratitude to the schools and students who participated.

Funding

This study was supported by the Health and Medical Research Fund, Food and Health Bureau, Hong Kong SAR Government (#02130486). The full report is available from the Health and Medical Research Fund website (<https://rfs1.fhb.gov.hk/index.html>).

Disclosure

The results of this research have been previously published in:

(1) Yu CCW, McManus AM, Au CT, et al. Appropriate scaling approach for evaluating peak VO_2 development in Southern Chinese 8 to 16 years old. *PLoS One* 2019;14:e0213674.

References

1. Sung RY, Yu CC, Choi KC, et al. Waist circumference and body mass index in Chinese children: cutoff values for predicting cardiovascular risk factors. *Int J Obes (Lond)* 2007;31:550-8.
2. Yu CCW, McManus AM, Li AM, Sung RYT, Armstrong N. Cardiopulmonary exercise testing in children. *Hong Kong J Paediatr (New Series)* 2010;15:35-47.
3. Cole TJ, Bellizzi MC, Flegal KM, Dietz WH. Establishing a standard definition for child overweight and obesity worldwide: international survey. *BMJ* 2000;320:1240-3.
4. McManus AM, Chung Yung T, Leung MP. Peak oxygen uptake in relation to age, sex, and maturation in Hong Kong Chinese children. *Am J Hum Biol* 2004;16:602-5.
5. Armstrong N, Welsman JR. Assessment and interpretation of aerobic fitness in children and adolescents. *Exerc Sport Sci Rev* 1994;22:435-76.

MicroRNA and its link to osteoblasts in adolescent idiopathic scoliosis: abridged secondary publication

JCY Cheng *, A Moreau, WYW Lee, TP Lam, BHK Yip, RKW Choy

KEY MESSAGES

1. Plasma miR-96 and miR-224 levels significantly increased in those with adolescent idiopathic scoliosis (AIS), compared with controls.
2. Plasma miR-96 and miR-224 correlated with bone quality parameters and bone turnover markers in AIS.
3. Aberrant level of miR-96 and miR-224 may contribute to abnormal osteoblast activities in AIS.

Hong Kong Med J 2020;26(Suppl 7):S10-2

HMRF project number: 04152176

JCY Cheng, A Moreau, WYW Lee, TP Lam, BHK Yip, RKW Choy

Department of Orthopaedics and Traumatology, The Chinese University of Hong Kong, Hong Kong

* Principal applicant and corresponding author: jackcheng@cuhk.edu.hk

Introduction

Adolescent idiopathic scoliosis (AIS) is a three-dimensional spinal deformity of unknown cause occurring predominantly in girls aged 10 to 13 years, with a global prevalence of 1% to 4%.¹ Severe curve deformity in AIS is associated with serious functional morbidities, cardiopulmonary compromise, early spinal degenerative changes, and psychosocial disturbance.² Bracing is the most recognised non-surgical treatment for skeletally immature patients with the Cobb angle between 25° and 40°, with a success rate of 70% to 75% subjected to good quality, compliance, adequate duration and monitoring.³ Age, Risser sign, and Cobb angle at initial visit, abnormal bone quality, and menarche have implication for curve progression, but their clinical use remains very limited.⁴ To search for more accurate biomarkers for evidence-based treatment of the high-risk group and to avoid unnecessary over-treatment and associated radiation exposure, we aimed to identify circulating biomarkers for diagnosis of AIS. It is speculated that abnormality of AIS bone metabolism results in vulnerable spine. Our previous study revealed a causative relationship between aberrant microRNA-145-5p (miR-145) expression and abnormal osteocyte structure and function associated with low bone mass and qualities in AIS.⁵ miRNAs are abundant in bio-fluids and their profiles are relatively stable for long-term clinical studies, thus rendering them as potential biomarkers for human diseases. Serological markers, such as circulating miRNA, might be an alternative indicator reflecting the abnormal bone metabolism in AIS.

This study consisted of two parts: (1) a retrospective case-control study to validate the plasma levels of the miRNA-96, -224, and -605 in AIS and healthy subjects; (2) an in vitro study

to elucidate the biological roles of miRNAs in osteoblast osteogenic activities in AIS using a primary osteoblasts culture model.

Methods

Ethical approval was obtained from the Joint Chinese University of Hong Kong – New Territories East Clinical Research Ethics Committee. Written informed consent was obtained from all subjects and their legal guardians. 100 girls with AIS (with Cobb angle evenly distributed from 15° to 80°) were recruited from the Scoliosis Clinic in Prince of Wales Hospital, Hong Kong, and 52 age-matched healthy girls were recruited randomly from local secondary schools as controls. Anthropometrical parameters (standing height, sitting height, body weight, and arm span) were measured with standard protocols. Cobb angle of the major curve was measured within a month before or after blood collection. Bone mineral density and bone qualities were assessed by dual-energy X-ray absorptiometry and high-resolution peripheral quantitative computed tomography, respectively. Serum samples were sent to Chan & Hou Medical Laboratories Ltd (Hong Kong) for assaying level of CTX/P1NP with Elecsys platform (Roche). miRNA level was tested in plasma with real-time PCR.

Iliac crest bone tissues were obtained from patients undergoing posterior instrumentation and spinal fusion requiring iliac crest autografts for AIS with a Cobb angle of >45°. Primary osteoblasts were isolated from bone biopsies. Human osteoblast cell line was used as control. Model of gain or loss of function in miR-96, -224, and -605 was constructed in primary AIS osteoblasts and control osteoblast cell line. mRNA level of representative osteogenic markers was assayed accordingly.

Results

Construction of miRNA signature in AIS

We assayed the expression level of miRNA candidates in plasma of the case-control cohort to construct the miRNA signature of AIS. Levels of miR-96 and miR-224 significantly increased in plasma of AIS, whereas miR-605 was undetectable in both plasma and serum. Area under the curve (AUC) analysis demonstrated discriminating potency of plasma miRNAs between AIS and healthy controls (unpublished data). Therefore, plasma miRNA signature of AIS composed of higher plasma levels of miR-96 and miR-224. Correlation analysis was conducted between the two miRNAs and clinical features in AIS, including Cobb angle, anthropometric information, serological bone metabolic markers, areal bone mineral density (measured with dual-energy X-ray absorptiometry), and bone quality parameters (measured with high-resolution peripheral quantitative computed tomography). Plasma levels of miR-96 and miR-224 in AIS showed correlation to certain bone quality parameters and serological bone turnover markers (CTx and

PINP). This indicates possible relation of plasma miRNA signature to the deranged bone qualities and metabolism in AIS.

Aberrant osteogenic differentiation of primary AIS osteoblasts

Osteoblasts in AIS showed consistently lower (but not significantly) alkaline phosphatase (ALP) activity in a temporal sequence (Fig. 1a). Calcium deposition capacity indicated by Alizarin Red staining showed significantly lower calcium nodules formation at day 14 under osteogenic induction in AIS osteoblast, compared with controls (Fig. 1b & 1c). In addition, AIS osteoblast differentially expressed representative osteogenic markers and exhibited significantly reduced mRNA expression of *Spp1*, *E11*, and *Opg* with osteogenic medium after 7 days culture. The *Rankl/Opg* ratio was consistently higher in AIS osteoblasts (Fig. 1d & 1e).

Regulation of miR-96, -224, -605 in osteogenic activities of osteoblast

Roles of miR-96, -224, -605 on osteoblast activities

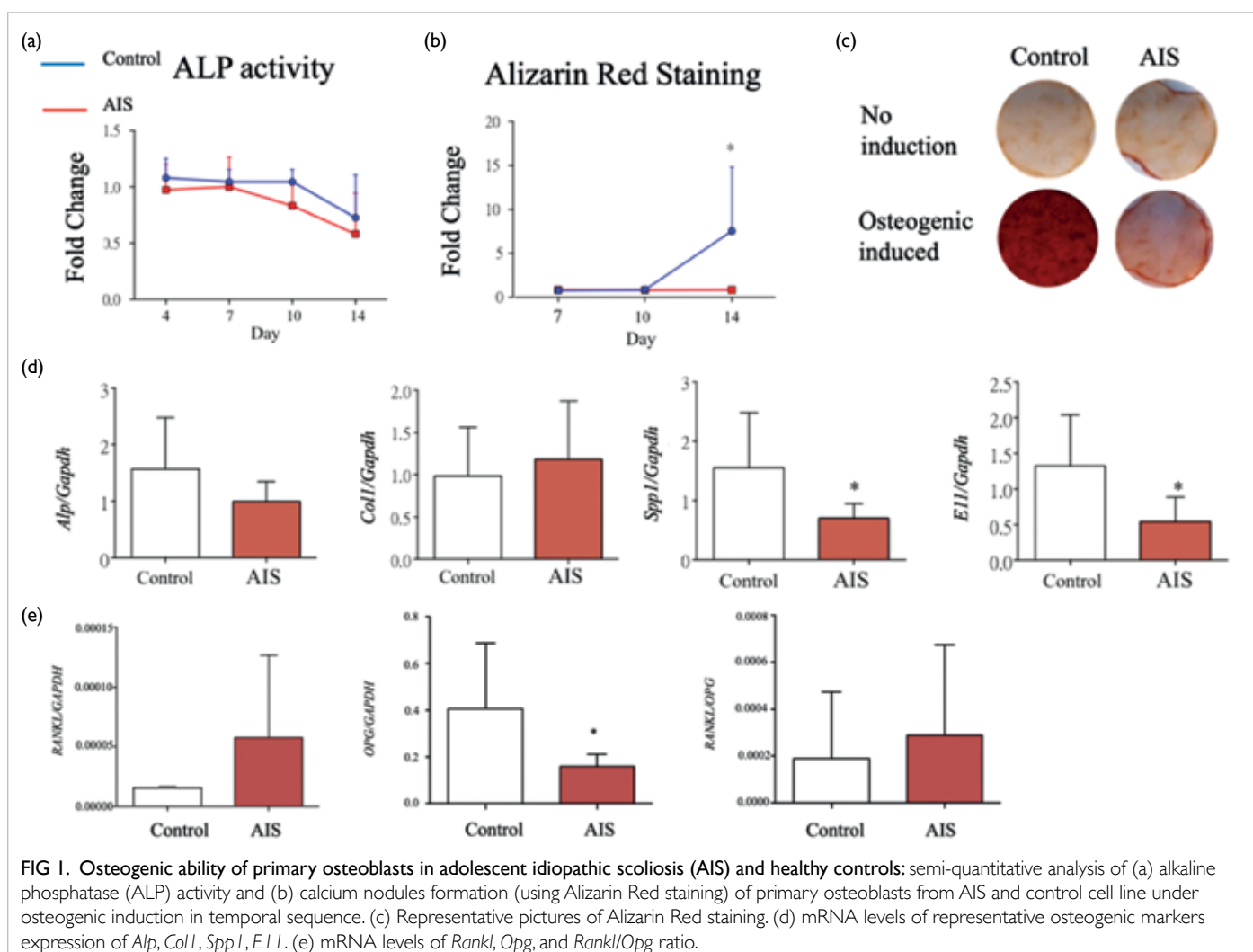


FIG 1. Osteogenic ability of primary osteoblasts in adolescent idiopathic scoliosis (AIS) and healthy controls: semi-quantitative analysis of (a) alkaline phosphatase (ALP) activity and (b) calcium nodules formation (using Alizarin Red staining) of primary osteoblasts from AIS and control cell line under osteogenic induction in temporal sequence. (c) Representative pictures of Alizarin Red staining. (d) mRNA levels of representative osteogenic markers expression of *Alp*, *Col1*, *Spp1*, *E11*. (e) mRNA levels of *Rankl*, *Opg*, and *Rankl/Opg* ratio.

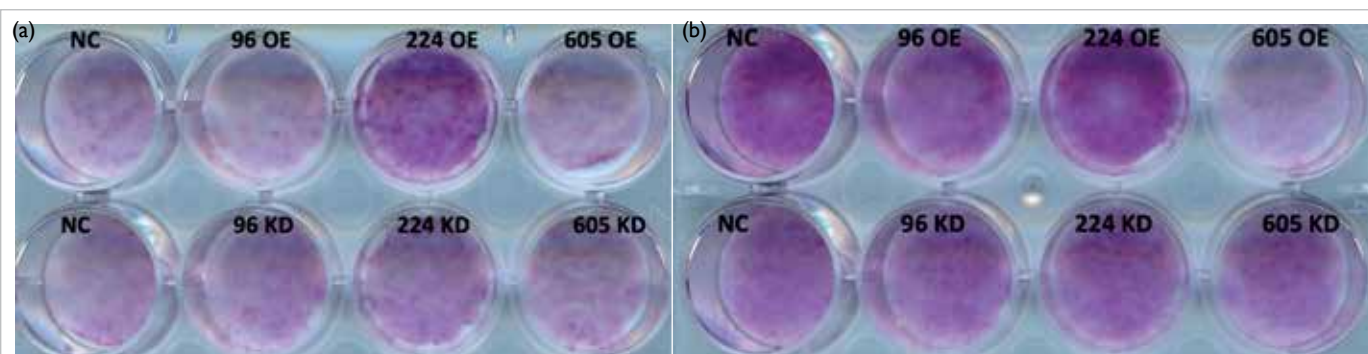


FIG 2. Representative pictures of alkaline phosphatase staining in gain or loss of function in osteoblasts cultured for 5 days in (a) basal medium and (b) osteogenic medium showing overexpression (OE) or knockdown (KD).

were shown in gain- or loss-of-function models in AIS primary osteoblast culture and control osteoblast cell line. Overexpression of miR-224 significantly increased ALP activity in osteoblasts after 5 days culture in basal medium (Fig. 2a). Overexpression of miR-605 significantly reduced ALP activity in osteoblasts after 5 days culture in osteogenic medium (Fig. 2b). mRNA level of representative markers for osteoblast activities were significantly changed in gain- or loss-of-function models.

Discussion

Our study aimed to investigate clinical implication of circulating miRNAs in disease diagnosis by determining associations between bone metabolism and underlying mechanism. Circulating miRNA signature of AIS was constructed from microRNA microarray of bone biopsies from AIS vs non-AIS control, and was validated in the plasma samples of a retrospective case-control cohort. miR-96 and miR-224 had significantly higher levels in AIS plasma and were correlated to the abnormal bone qualities in AIS. Plasma levels of miR-96 and miR-224 had significantly positive correlation with serum levels of P1NP and CTx in AIS. This correlation pattern suggested that miR-96 and miR-224 can be used to reflect bone turnover and pathological alteration of bone cell biology in AIS. In vitro study provided evidence for regulation of miR-96, -224, and -605 in osteogenic activities in osteoblasts with gain- or loss-of-function model. Our study proposed an evidence-based diagnosis of circulating miRNAs to aid decision making in management for AIS. The results enable construction of a model with pathology-associated clinical features and differentially expressed miRNAs. This study is the first step for constructing a reliable predictive system of curve progression at the early presentation of AIS using validated biomarkers and clinical features.

Conclusion

Plasma miRNAs was potential biomarkers to

distinguish AIS from healthy controls.

Funding

This study was supported by the Health and Medical Research Fund, Food and Health Bureau, Hong Kong SAR Government (#04152176). The full report is available from the Health and Medical Research Fund website (<https://rfs1.fhb.gov.hk/index.html>).

Disclosure

The results of this research have been previously published in:

1. Zhang J, Chen H, Leung RKK, et al. Aberrant miR-145-5p / β -catenin signal impairs osteocyte function in adolescent idiopathic scoliosis. *FASEB J* 2018;fj201800281.
2. Chen H, Zhang J, Wang Y, et al. Abnormal lacuna-canalicular network and negative correlation between serum osteocalcin and Cobb angle indicate abnormal osteocytes function in adolescent idiopathic scoliosis. *FASEB J* 2019;33:13882-13892.
3. Zhang J, Cheuk KY, Xu L, et al. A validated composite model to predict risk of curve progression in adolescent idiopathic scoliosis. *EClinicalMedicine* 2020;18:100236.

References

1. Cheng JC, Castelein RM, Chu WC, et al. Adolescent idiopathic scoliosis. *Nat Rev Dis Primers* 2015;1:15030.
2. Weinstein SL, Dolan LA, Cheng JC, Danielsson A, Morcuende JA. Adolescent idiopathic scoliosis. *Lancet* 2008;371:1527-37.
3. Richards BS, Bernstein RM, D'Amato CR, Thompson GH. Standardization of criteria for adolescent idiopathic scoliosis brace studies: SRS Committee on Bracing and Nonoperative Management. *Spine (Phila Pa 1976)* 2005;30:2068-77.
4. Noshchenko A, Hoffecker L, Lindley EM, et al. Predictors of spine deformity progression in adolescent idiopathic scoliosis: a systematic review with meta-analysis. *World J Orthop* 2015;6:537-58.
5. Zhang J, Chen H, Leung RKK, et al. Aberrant miR-145-5p/ β -catenin signal impairs osteocyte function in adolescent idiopathic scoliosis. *FASEB J* 2018;fj201800281.

Home-based exercise intervention for caregivers of persons with dementia: a randomised controlled trial: abridged secondary publication

WC Chan *, LCW Lam, N Lautenschlager, B Dow, SL Ma

KEY MESSAGES

1. Home-based structured exercise programme (12-step sitting Tai Chi) alleviates mild depressive symptoms among caregivers of persons with dementia.
2. Sitting Tai Chi also improves the balance ability of both caregivers and care recipients, and immediate word-list recall of care recipients.
3. As a traditional mind-body exercise widely practised by local older adults, sitting Tai Chi offers a low cost and safe treatment option for mild depressive symptoms in caregivers.

Hong Kong Med J 2020;26(Suppl 7):S13-6

HMRP project number: 11121441

¹ WC Chan, ² LCW Lam, ^{3,4,5} N Lautenschlager, ⁶ B Dow, ² SL Ma

¹ Department of Psychiatry, The University of Hong Kong

² Department of Psychiatry, The Chinese University of Hong Kong

³ Academic Unit for Psychiatry of Old Age, Department of Psychiatry, University of Melbourne, Melbourne, Australia

⁴ NorthWestern Aged Mental Health, Royal Park Campus, Parkville, Australia

⁵ School of Clinical Neurosciences and the Western Australia Centre and Health and Ageing, University of Western Australia, Perth, Australia

⁶ National Ageing Research Institute, The University of Melbourne, Melbourne, Australia

* Principal applicant and corresponding author: waicchan@hku.hk

Introduction

In Hong Kong, around one in 10 older persons is estimated to have dementia.¹ Informal caregivers who provide most of dementia care experience considerable stress.² Evidence suggests that dementia caregivers are at an elevated risk of developing depression and anxiety and report poorer quality of life. They also have poorer perceived health, higher risk of hypertension, lower immunity, and elevated risk of mortality. We compared the efficacy of a home-based structured exercise programme (12-step sitting Tai Chi) for both carers and care recipients with a non-exercise social contact control group in the treatment of depression among caregivers of persons with dementia.

Methods

This assessor-blind randomised controlled study comprised an intervention phase of 12 weeks and an extended observation phase of another 12 weeks. Participants were recruited from various district elderly community centres, neighbourhood elderly centres, and psychogeriatric and geriatric clinics in Hong Kong. Ethics approval was obtained from the institutional review boards; written informed consent was obtained from each participant. Inclusion criteria for informal caregivers were age ≥ 50 years, providing a substantial amount of care for the persons with dementia, having a score of >0 to <8 in the 15-item Geriatric Depression Scale, receiving antidepressant treatment on a steady dose for at least 3 months (if applicable), and understanding

Chinese. Inclusion criteria for care recipients were age ≥ 60 years, clinically diagnosed with dementia, dependence in at least one of the activities of daily living, having Mini Mental State Examination (MMSE) score of >10 , and understanding Chinese. Exclusion criteria for both were having regular (≥ 3 times/week) Tai Chi practice or other forms of mind-body exercise such as yoga, qigong, or mindfulness training in the past 6 months, presence of any condition that rendered participants unsuitable for physical training such as severe psychotic symptoms, imminently suicidal, significant orthopaedic problems, or unstable medical conditions.

Block randomisation was used. Team member was not involved in subsequent assessment or training. The assessors for clinical parameters were blinded to participants' randomisation status, and the trainers were blinded to the assessment results.

Intervention consisted of eight home-based sessions on 12-step sitting Tai Chi.³ Each session lasted for 1 hour conducted by a Tai Chi teacher who visited the dyads in their home weekly in the first 4 weeks, followed by biweekly over the next 8 weeks. In addition, bi-weekly phone contacts were made (ie, 12 scheduled phone contacts in 24 weeks) to monitor the progress and address participants' concerns.

Because social contact may be beneficial to one's mood and may contribute to any improvement observed in the intervention group, we provided participants in the control group with a level of social contact equivalent to the intervention group. Participants in control group were visited by the

research assistant for eight times over 12 weeks. The visits involved a series of conversations related to neutral non-exercise topics that were designed according to the principles of a befriending programme. Similarly, 12 bi-weekly phone calls were made to offer a comparable level of social contact.

The primary outcome measure was the proportion of caregivers who were classified as responders by Hamilton Rating Scale for Depression (HAM-D-17). Secondary outcome measures included MMSE, digit span, immediate and delayed word-list recall, category verbal fluency test, Berg Balance Scale (BBS), exercise logbook and pedometer record, and brain-derived neurotrophic factor polymorphisms. Secondary outcome measures for caregivers only included Zarit Carer Burden Interview, Short Form-12 Health Survey (SF-12), Executive Interview, relevant items extracted from International Personality Item Pool, and qualitative data by focus group interviews.

Secondary outcome measures for care recipients only were Neuropsychiatric Inventory, Disability Assessment for Dementia, Modified Barthel Index, and Cornell Scale for Depression in Dementia.

Results

Of 262 caregiver-care recipient dyads screened for eligibility, 46 refused to participate and 79 did not fulfil the inclusion criteria. Among the 137 dyads who met inclusion criteria, 27 (19.7%) dyads dropped out owing to time constraints (n=13), six dyads refused to continue as they were unsatisfied with the randomisation results, seven dyads left because of physical illnesses or procedures not related to exercise, and one care recipient in the control group died after a fall (Fig. 1).

The mean age of care recipients was 80.7±7.2 years. Half of them were men. Nearly 80% were illiterate or had education up to primary level. Their mean time in education was 4.4±4.4 years. Their mean MMSE score was 19.9±4.6. The overall mean Neuropsychiatric Inventory score was 5.1±9.3 and the mean Disability Assessment for Dementia score was 68.8%±24.9%. The two groups were comparable at baseline.

The mean age of caregivers was 68.2±10.7 years, and there was a female preponderance. Nearly two-thirds of the caregivers were spouses of the care recipients, and one-third were their grown-up children. Their mean time in education was 7.9±5.5 years. Their mean MMSE score was 28.6±2.1. Caregivers spent a mean of 7.6±6.3 hours daily to care. The mean length of caregiving was 4.5±3.6 years. The overall mean Geriatric Depression Scale score was 4.1±2.3. There was no significant difference in sociodemographic and clinical characteristics between the two groups. Group × time interaction on BBS scores was found at week 12 in the sitting Tai Chi group but no significant change in the control group ($\beta=1.34, P=0.044$, Table).

At week 12, 49.1% of the caregivers in sitting Tai Chi group achieved a reduction of ≥50% in HAM-D-17, whereas 29.6% of those in the control group had the same reduction (Table). In a multivariate model adjusted for age, sex, education, and baseline depression severity, sitting Tai Chi was associated with a reduction in caregiver depression (odds ratio=2.55, 95% confidence interval=1.09-5.97, $P=0.031$). However, the beneficial effect of sitting Tai Chi did not sustain at week 24.

Linear mixed-effects analysis demonstrated significant effects of group × time interaction on HAM-D-17 scores in the sitting Tai Chi group at week 6 ($\beta= -1.38, P=0.032$) and week 12 ($\beta= -0.90, P=0.030$) [Fig. 2]. Group × time interaction on BBS scores was found at week 12 in the sitting Tai Chi group but no significant change in the control group ($\beta=3.32, P=0.029$, Table). Significant effects of

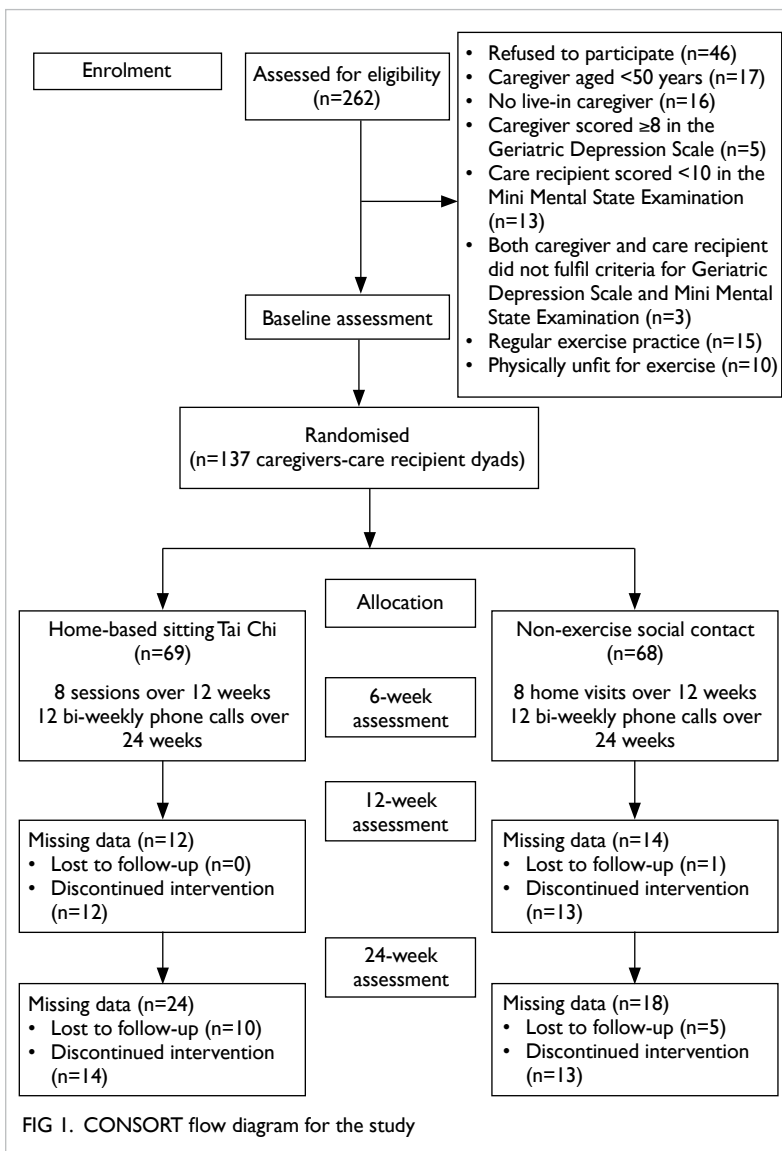
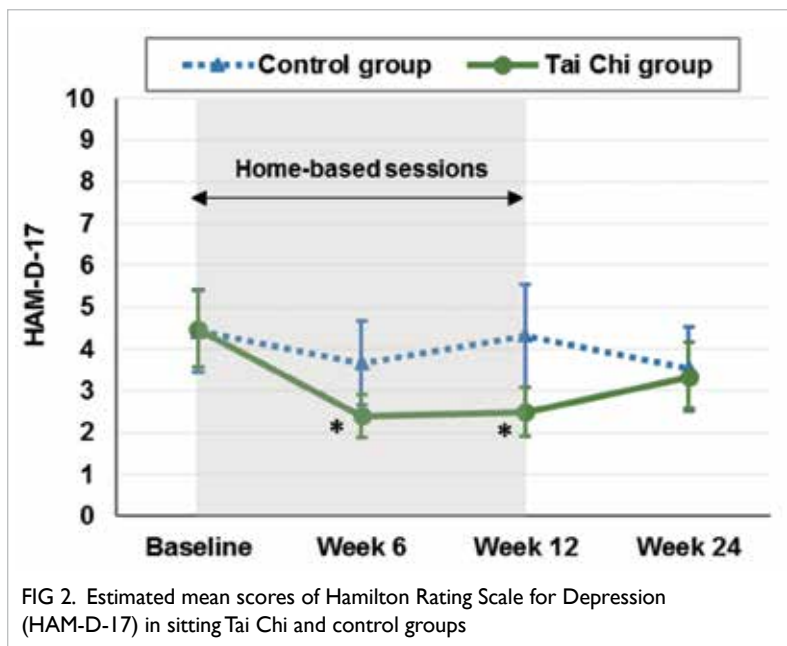


TABLE. Mood, behavioural, functional, and physical outcomes of informal caregivers and care recipients

Assessment	Sitting Tai Chi group*	Non-exercise social contact group*	Group × time interaction effects		
			Beta (SE)	95% CI	P value
Informal caregivers					
Hamilton Rating Scale for Depression					
Baseline	4.48±3.88	4.43±4.11			
Week 6	2.40±1.92	3.67±3.74	-1.38 (0.63)	-2.63 to -0.12	0.032
Week 12	2.49±2.25	4.31±4.60	-0.90 (0.41)	-1.71 to -0.09	0.030
Week 24	3.33±2.84	3.54±3.50	-0.19 (0.39)	-0.96 to 0.57	>0.05
Zarit Carer Burden Interview					
Baseline	30.57±17.81	31.49±17.09			
Week 6	26.70±15.44	27.37±13.22	-0.21 (2.16)	-4.49 to 4.08	>0.05
Week 12	29.05±17.90	29.30±18.17	0.15 (1.90)	-3.60 to 3.90	>0.05
Week 24	31.58±18.55	29.86±16.36	1.01 (0.87)	-0.71 to 2.73	>0.05
Physical Component Summary					
Baseline	46.74±9.28	45.23±9.01			
Week 12	48.90±8.90	46.21±9.22	1.08 (0.99)	-1.72 to 1.94	>0.05
Week 24	47.02±9.02	46.55±9.17	0.78 (0.67)	-1.02 to 1.65	>0.05
Mental Component Summary					
Baseline	52.22±7.34	53.01±6.66			
Week 12	54.01±7.21	53.95±6.68	0.87 (0.67)	-4.90 to 3.87	>0.05
Week 24	53.33±7.43	53.87±6.92	0.62 (0.59)	-4.46 to 3.99	>0.05
Berg Balance Scale					
Baseline	52.59±5.54	53.48±5.01			
Week 12	53.63±4.64	53.27±6.13	1.34 (0.66)	0.04 to 2.64	0.044
Week 24	53.47±4.33	53.90±4.19	0.53 (0.58)	-0.61 to 1.66	>0.05
Care recipients					
Cornell Scale for Depression in Dementia					
Baseline	0.80±1.24	1.30±2.24			
Week 6	0.50±1.30	0.93±1.61	-0.05 (0.30)	-0.64 to 0.53	>0.05
Week 12	0.46±1.44	0.57±1.10	0.12 (0.18)	-0.22 to 0.47	>0.05
Week 24	0.27±0.86	0.67±1.34	0.01 (0.14)	-0.27 to 0.30	>0.05
Neuropsychiatric Inventory					
Baseline	4.28±7.93	5.90±10.52			
Week 12	3.95±9.35	5.62±12.28	-1.63 (1.61)	-4.81 to 1.56	>0.05
Week 24	5.29±11.54	4.52±9.73	-0.27 (1.14)	-2.52 to 1.98	>0.05
Disability Assessment for Dementia					
Baseline	68.76±21.45	68.90±28.24			
Week 12	67.82±22.81	66.17±31.32	3.57 (3.09)	-2.56 to 9.71	>0.05
Week 24	67.46±26.69	70.73±25.53	0.31 (2.45)	-4.63 to 5.25	>0.05
Modified Barthel Index					
Baseline	77.96±21.58	73.37±27.58			
Week 12	75.84±24.48	70.81±28.03	1.11 (3.55)	-6.33 to 8.56	>0.05
Week 24	79.41±23.75	76.52±24.08	-0.34 (2.39)	-5.11 to 4.44	>0.05
Berg Balance Scale					
Baseline	42.06±10.80	40.69±15.67			
Week 12	46.02±8.35	43.77±12.31	3.32 (1.49)	0.35 to 6.29	0.029
Week 24	44.15±11.12	43.28±12.76	2.43 (1.31)	-0.28 to 5.15	>0.05

* Data are presented as mean ± standard deviation



group \times time interaction on immediate word-list recall was found in the sitting Tai Chi group at both week 12 ($\beta=0.82$, $P=0.033$) and week 24 ($\beta=0.62$, $P=0.014$) [Table].

Discussion

Our study showed that sitting Tai Chi alleviated depressive symptoms among caregivers of persons with dementia. The results are in line with the literature that physical exercise alleviates depressive symptoms. In two meta-analyses of 23 and 25 randomised controlled trials, physical exercise was proven to be an effective intervention for depression.^{4,5} Nonetheless, most previous studies examined the efficacy of walking/running/jogging, aerobic exercise, strength training, and stationary bicycle/ergometer training, all of which may not suit the needs of older adults. Findings of the current study validated the efficacy of the sitting Tai Chi (a traditional mind-body exercise) in older adults.

Apart from the psychological benefits, sitting Tai Chi also improved balance ability among caregivers and care recipients, as exemplified by their BBS scores. This is a potentially important finding because falls is a cause of injury-related death and non-fatal injuries among those aged ≥ 65 years. Sitting Tai Chi, by improving participants' balancing ability, might reduce their risk of falls. Its beneficial effects on balance ability may be attributed to the fact that participants in the intervention group took up more physical activities.

Furthermore, sitting Tai Chi improved

immediate word-list recall among care recipients at the end of intervention (week 12) and extended observation period (week 24). However, there was no significant change in other cognitive domains among participants in the intervention group. It may be due to the fact that sitting Tai Chi is less intense than standard 24-step Tai Chi, and the intervention consisted of eight home-based sessions over 12 weeks only. Interventions of higher frequency and longer duration may be required to achieve improvement in other cognitive domains. Further studies will be required to determine the optimal dosage of exercise for this population.

Acknowledgements

We would like to thank the participants for their kind support. We would also like to express our sincere thanks to our Tai Chi teacher Mr Charles Lee, and the social centres and clinics for their valuable support in participant recruitment. In addition, we are grateful to Mrs Eleanor Chan and Mrs Miranda Tung for their advice on the assessment methods.

Funding

This study was supported by the Health and Medical Research Fund, Food and Health Bureau, Hong Kong SAR Government (#11121441). The full report is available from the Health and Medical Research Fund website (<https://rfs1.fhb.gov.hk/index.html>).

Disclosure

The results of this research have been previously published in:

1. Chan WC, Lautenschlager N, Dow B, Ma SL, Wong CS, Lam LC. A home-based exercise intervention for caregivers of persons with dementia: study protocol for a randomised controlled trial. *Trials* 2016;17:460.

References

1. Lam LC, Tam CW, Lui VW, et al. Prevalence of very mild and mild dementia in community-dwelling older Chinese people in Hong Kong. *Int Psychogeriatr* 2008;20:135-48.
2. Chan WC, Ng C, Mok CC, Wong FL, Pang SL, Chiu HF. Lived experience of caregivers of persons with dementia in Hong Kong: a qualitative study. *East Asian Arch Psychiatry* 2010;20:163-8.
3. Lee KY, Jones AY, Hui-Chan CW, Tsang WW. Kinematics and energy expenditure of sitting t'ai chi. *J Altern Complement Med* 2011;17:665-8.
4. Kvam S, Kleppe CL, Nordhus IH, Hovland A. Exercise as a treatment for depression: a meta-analysis. *J Affect Disord* 2016;202:67-86.
5. Schuch FB, Vancampfort D, Richards J, Rosenbaum S, Ward PB, Stubbs B. Exercise as a treatment for depression: a meta-analysis adjusting for publication bias. *J Psychiatr Res* 2016;77:42-51.

Nanoparticles to identify Alzheimer disease by magnetic resonance imaging: abridged secondary publication

L Baum, AHL Chow *, YX Wang, EX Wu, RG Pautler

KEY MESSAGES

1. We designed and tested an imaging material that can be used to detect Alzheimer disease (AD) by magnetic resonance imaging (MRI).
2. The material consists of magnetic iron nanoparticles coated with curcumin that binds the amyloid plaques in AD brain.
3. After injecting the nanoparticles, MRI distinguished AD from control model mice.
4. In examining slices of brains, the nanoparticles were highly concentrated at the plaques and significantly coincided with the dark spots seen on MRI.

5. The nanoparticles were non-toxic to cells grown in dishes.

Hong Kong Med J 2020;26(Suppl 7):S17-9

HMRF project number: 01120556

¹ L Baum, ¹ AHL Chow, ² YX Wang, ³ EX Wu, ⁴ RG Pautler

¹ School of Pharmacy, The Chinese University of Hong Kong

² Department of Imaging and Interventional Radiology, The Chinese University of Hong Kong

³ Department of Electrical and Electronic Engineering, The University of Hong Kong

⁴ Department of Molecular Physiology and Biophysics, Baylor College of Medicine, Texas, USA

* Principal applicant and corresponding author: mrpharms009@gmail.com

Introduction

Alzheimer disease (AD) is an incurable and progressive neurodegenerative disorder.^{1,2} Current AD drugs only provide partial symptomatic relief and do not slow degeneration. Some drug candidates may prove effective in delaying disease progression.^{1,2} However, large clinical trials have failed to show efficacy of the drug candidates in AD; there were only trends toward effectiveness among patients with mild AD. The current consensus is that the failure was not an inability of the drugs to accomplish their molecular action, but was a matter of timing: treatment beginning too late, after loss of brain function.^{1,2} Therefore, it is important to identify patients as early as possible to initiate treatment before irreversible brain injury takes place.

Positron emission tomography enables early diagnosis of AD by detecting amyloid plaques with a radioactive compound that binds plaques. However, this method is very expensive and is only available near a cyclotron that can generate the radioactively labelled reagent. Only one site in Hong Kong offers this service. Therefore, only limited patients may benefit from early diagnosis and potential treatment.

Magnetic resonance imaging (MRI) is more affordable and widely available. We aim to develop a method of labelling amyloid plaques for MRI. We developed magnetic particles that can enter the brain and specifically bind to amyloid plaques for detection by MRI. The particles consist of a microscopic iron core coated with curcumin (a natural compound) and polymers (long molecules

used in some drugs and foods). The curcumin binds both iron and amyloid plaques, thus temporarily anchoring the particles to plaques in the brain. The polymers protect the particles circulating in the blood. Curcumin can reach the brain and bind plaques in mice,³ and iron particles have been used for several MRI applications.⁴

Early diagnosis of AD enables early treatments; if effective, patient ability to function independently may be preserved, thus extending the duration of healthy life and reducing the burden on caregivers and costs to healthcare system. Preventive treatments, to be effective, must couple with cost-effective early diagnosis.

Methods

AD model mice and their normal siblings were used. Iron solutions were mixed under certain conditions to make a black powder consisting of nanoparticles. Curcumin and polymers were added to coat the nanoparticles. Their size, electric charge, and structure were analysed using several methods.

To determine whether the nanoparticles were safe to cells, cells were grown in dishes and nanoparticles were added. We then measured a chemical the cells produce when they are healthy; the amount of the chemical indicates the health of the cells. To determine whether the nanoparticles can enter the brain, we added them to liquid on one side of a layer of cells and measured the nanoparticles that crossed the layer to the liquid on the other side.

Some mice were injected with nanoparticles

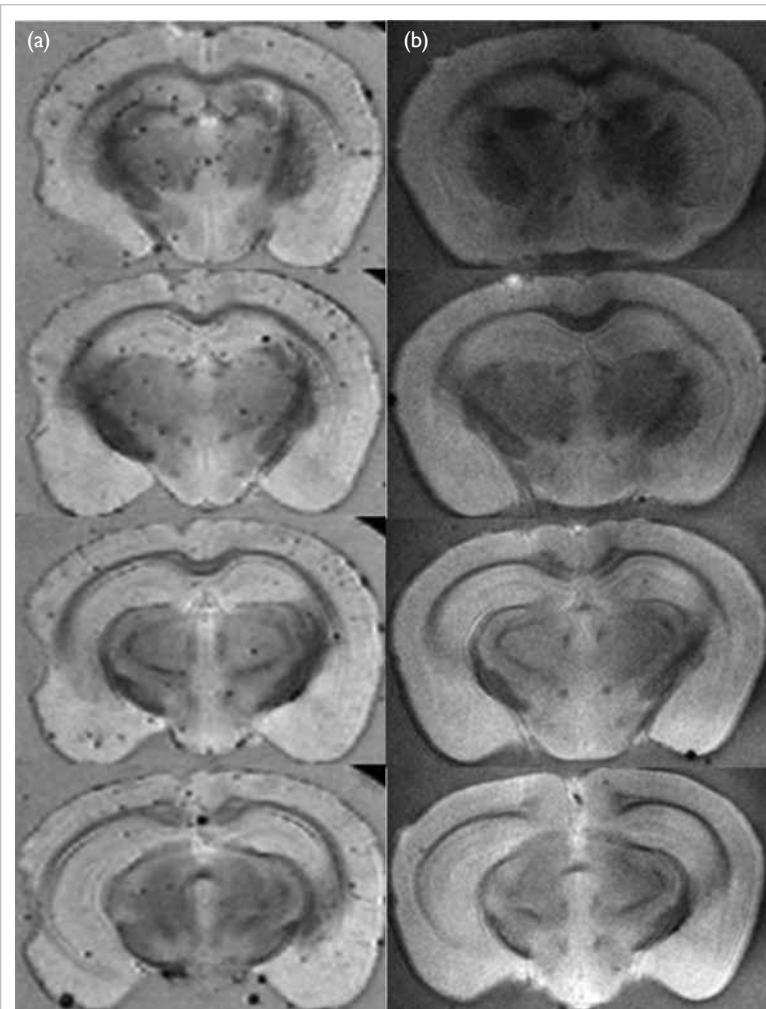


FIG 1. Magnetic resonance images of brains after nanoparticle injection and brain removal in (a) mice with Alzheimer disease and (b) normal mice

and then killed after 1, 3, 5, or 24 hours to assess distribution of iron in different organs.

The nanoparticles were injected into AD mice and their normal siblings. After 4 hours, mice were scanned by MRI and then killed, and their brains were removed and scanned again by MRI. The area covered by dark spots in MRI was measured.

Brains were thinly sliced and stained to show plaques (red) and iron (blue), and fluorescence showed curcumin (yellow).

To determine safety, memory of mice was tested 2 days after injecting nanoparticles.

Results

The mean diameter of nanoparticles was <100 nm. Their electric charge was almost neutral. X-ray analysis confirmed that the nanoparticles contained iron. Infrared analysis suggested that curcumin bound iron, and that polymers coated the nanoparticles. Baking off the coating of the nanoparticles left 14% of their weight, representing the iron. Another X-ray method supported the known structure of the nanoparticles: the middle containing iron and the outer layers containing carbon, a component of curcumin and polymers.

The nanoparticles were safe to cells. They crossed a layer of cells at a steady rate, suggesting that they may also be able to enter the brain.

After injecting nanoparticles into AD and normal mice, iron concentration rose in blood and brain but not in other organs tested (except for liver at 1 hour). We chose to perform MRI 4 hours after injection because 4 hours seemed likely to show the minimum non-specific binding in the brain.

After injecting nanoparticles, MRI showed significantly more dark spots in AD mice than in normal mice (Fig. 1), both before and after extracting the brains. Dark spots were concentrations of nanoparticles at amyloid plaques (Fig. 2). Without curcumin, iron particles do not show the increased plaques expected in AD mice. Young mice, which have few plaques, also showed more dark spots in AD mice than in normal mice.

In brain slices from mice injected with nanoparticles, amyloid plaques often appeared in the same places as the nanoparticles and dark spots in matching MRI images (Fig. 3).

The memory of mice given the nanoparticles 2 days before did not significantly differ from that of mice not given the nanoparticles.

Discussion

An ideal nanoparticle should be stable and small (<100 nm) to get through tiny blood vessels and remain in the blood long enough to enter the brain. It should reach the brain and bind amyloid plaques. It should be safe to cells and animals. Our

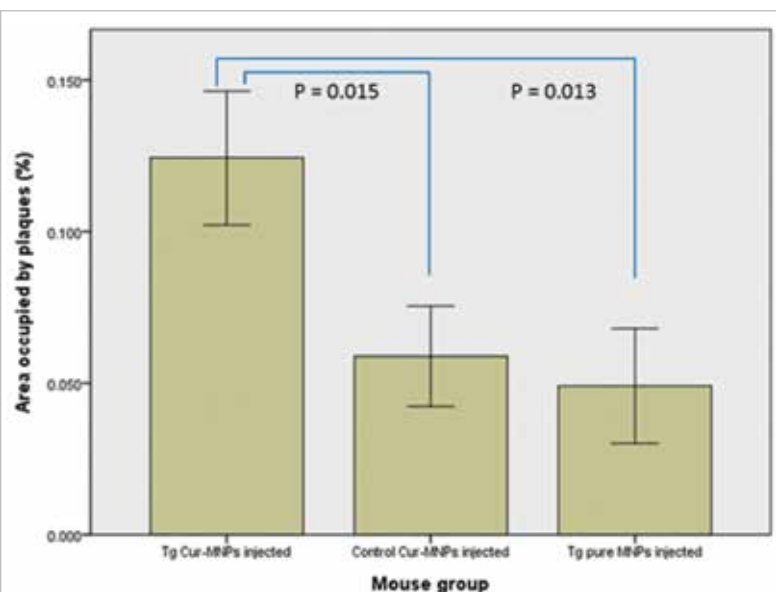


FIG 2. Area occupied by plaques in magnetic resonance images of live mice after injecting nanoparticles in Alzheimer disease mice (left), normal mice (middle), and Alzheimer disease mice after injecting iron particles without curcumin (right)

nanoparticles have these desired attributes.

Multiple methods confirmed that the nanoparticles have the predicted structure: a core of iron, a layer of curcumin, and an outer layer of polymers. The polymers lent particles longevity in the blood and ability to penetrate the blood-brain barrier. The nanoparticles were safe to cells and could penetrate a cell monolayer. Thus, the nanoparticles may be able to enter the brain. We chose 4 hours as the time for MRI imaging because non-specific binding appears to be minimised at around that time.

MRI and brain slices proved that the nanoparticles entered the brain and bound to plaques. MRI of AD mice displayed significantly more black spots, representing nanoparticles. This occurred even in young mice, with few plaques. Thus, nanoparticles may help detect AD early. They can be further tested in human clinical trials in the future.

Acknowledgements

We thank Prof Robert Prud'homme, Department of Chemical and Biological Engineering, University of Princeton, and Professor Christopher Macosko, Department of Chemical Engineering and Materials Science, University of Minnesota, for their kind assistance in fabricating a multi-inlet vortex mixer. We also thank Erica Leung for image analysis and data processing.

Funding

This study was supported by the Health and Medical Research Fund, Food and Health Bureau, Hong Kong SAR Government (#01120556). The full report is available from the Health and Medical Research Fund website (<https://rfs1.fhb.gov.hk/index.html>).

Disclosure

The results of this research have been previously

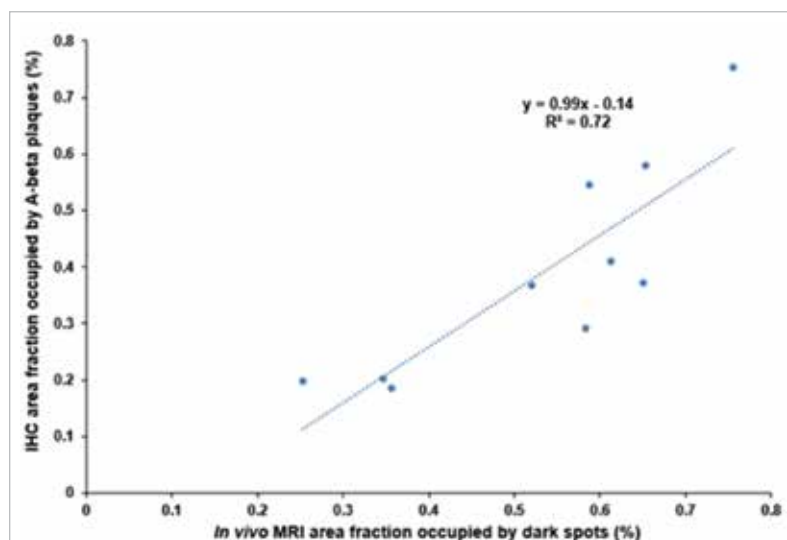


FIG 3. Areas of plaques in brain slices of Alzheimer disease mice correlate with area of nanoparticles in corresponding magnetic resonance images

published in:

1. Cheng KK, Chan PS, Fan S, et al. Curcumin-conjugated magnetic nanoparticles for detecting amyloid plaques in Alzheimer's disease mice using magnetic resonance imaging (MRI). *Biomaterials* 2015;44:155-72.

References

1. Chiang K, Koo EH. Emerging therapeutics for Alzheimer's disease. *Annu Rev Pharmacol Toxicol* 2014;54:381-405.
2. Briggs R, Kennelly SP, O'Neill D. Drug treatments in Alzheimer's disease. *Clin Med (Lond)* 2016;16:247-53.
3. Yang F, Lim GP, Begum AN, et al. Curcumin inhibits formation of amyloid beta oligomers and fibrils, binds plaques, and reduces amyloid in vivo. *J Biol Chem* 2005;280:5892-901.
4. Wang YX. Superparamagnetic iron oxide based MRI contrast agents: current status of clinical application. *Quant Imaging Med Surg* 2011;1:35-40.

Targeted drug discovery for Alzheimer disease: abridged secondary publication

AML Chan *, L Baum, RCC Chang, JA Esteban, ZX Lin, YH Wong, WH Yung

KEY MESSAGES

1. We identify a small molecule, ZL006, that possesses therapeutic effects by alleviating memory deficits in a mouse model of Alzheimer disease.
2. The therapeutic effects of ZL006 in enhancing learning and memory are likely due to its ability in blocking PTEN-mediated pathological events in synapses.
3. The mechanism of action of ZL006 is likely due to restoration of synaptic function but not by promoting neuronal survival.
4. ZL006 has the potential in treating early stage Alzheimer disease.

Hong Kong Med J 2020;26(Suppl 7):S20-2

HMRF project number: 02130026

¹ AML Chan, ² L Baum, ¹ RCC Chang, ³ JA Esteban, ⁴ ZX Lin, ⁵ YH Wong, ¹ WH Yung

¹ School of Biomedical Sciences, The Chinese University of Hong Kong

² School of Pharmacy, The Chinese University of Hong Kong

³ Department of Molecular Neurobiology, Centro de Biología Molecular 'Severo Ochoa', Consejo Superior de Investigaciones Científicas (CSIC), Spain

⁴ School of Chinese Medicine, The Chinese University of Hong Kong

⁵ Division of Life Science, The Hong Kong University of Science and Technology

* Principal applicant and corresponding author: andrewmchan@cuhk.edu.hk

Introduction

Alzheimer disease (AD) is an irreversible, progressive brain disorder that destroys memory and cognitive skills. The cumulative deposit of β -amyloid plaques and neurofibrillary tangles in the brain are considered the hallmarks of AD. The pathological mediator is a short 42 amino acids amyloid beta ($A\beta$) peptide. $A\beta$ can perturb two forms of neuroplasticity. Indeed, enhanced long-term depression (LTD) and impaired long-term potentiation (LTP) accompanied by dendritic spine elimination and neuron loss could be elicited by acute $A\beta$ treatment.¹ There are two classes of medication for AD: cholinesterase inhibitors and N-methyl-d-aspartate receptor inhibitors. However, the two types of drugs could only relieve the memory deficits in a very short period without any modification or delay in the progression of the disease.

Phosphatase and tensin homologue deleted from chromosome 10 (PTEN) is a lipid phosphatase with specificity towards phosphatidylinositol-3,4,5-trisphosphate. PTEN is a key negative regulator of the phosphoinositide 3-kinase/mammalian target of rapamycin signalling pathway.² The 403-amino acid PTEN protein harbours a PSD-95/Dlg1/ZO-1 (PDZ)-binding domain, which comprises four amino acids: Ile-Thr-Lys-Val. PDZ domain containing proteins often show interaction with the C-terminus of its binding partner PDZ-binding domain (PDZ-BD), especially in postsynaptic density (PSD). PSD-95 is one of the most abundant scaffolding protein involved in synaptic strengths and PSD architecture maintenance.

Previous studies have implicated PTEN involvement in N-methyl-d-aspartate receptor-dependent LTD, whereas basal synaptic transmission, LTP, mGluR-dependent LTD, and presynaptic paired-pulse facilitation are not affected.³ The process of LTD induction is accompanied by the interaction between PTEN and PSD-95, which leads to the recruitment and anchoring of PTEN at the PSD in dendrite spines.³ PTEN is recruited to the dendritic spines following treatment with $A\beta$. Moreover, this kind of recruitment is in a PDZ-BD-dependent manner. In other words, deletion of PDZ-BD results in the reduction in the level of PTEN recruited to the dendritic spines. Indeed, both $A\beta$ -elicited abnormal LTD and LTP are abolished in the acute hippocampal slice derived from mice that lack PTEN PDZ-BD.⁴

We hypothesised that the blocking of the interaction between PTEN and PSD-95 could restore synaptic plasticity, and cognitive impairment would be alleviated in patients with AD. The aim of this study was to screen for compounds that can block the action of PTEN. Lead compounds would then be tested for their ability to alleviate cognitive impairments in a mouse model of AD.

Methods

Fluorescence polarisation

To screen for potential small molecule inhibitors, a fluorescent-labelled peptide FITC-PFDEDQHTQITKV-COOH was used as a fluorescent probe. A range of concentrations, 10 nM to 72 μ M, of the fusion protein of GST-PSD-95 PDZ2

was incubated with 5 μM (for compound screening) or 10 μM (for standard curve) peptide for 30 minutes at 4°C. The extent of polarisation was measured on a SpectraMax i3 instrument. For compound screening, the compounds were added after the initial incubation, each mixture was incubated for 30 minutes at 4°C, the reaction mixture was assayed in the same way as for the standard curve.

Behavioural tests

Male 5XFAD transgenic mice aged 6 to 7 months were used as a model of AD. The Morris water maze test was performed at a pre-training day (day 0), 4 training days (days 1-4), and a probe trial day (day 5). The average of five trials was calculated to give a single path length and escape latency on each day for each mouse. For day 5, single values for the path length, escape latency, and time spent in the platform quadrant and tank for each mouse were collected. Data were analysed using two-way ANOVA.

Results

To identify small molecules that could inhibit the binding between PTEN PDZ-BD and the PDZ2 domain of PSD-95, we performed an *in silico* screening of a chemical library (ChemDiv; San Diego [CA], USA) of 4094 compounds with structural features that can dock the PSD-95 PDZ-2 binding pocket, and a docking score was calculated for each compound, with 60 highest-scored compounds selected for further validation. In addition, ZL006, which has been shown to disrupt ischaemia-induced nNOS and PSD-95 interaction, was also included for further investigation.⁵

Fluorescence polarisation is a biochemical assay for measuring the affinity of the interaction between a small ligand and its interacting protein of a greater mass. Fluorescent-labelled ligands in solution have a scattered emission profile when excited. However, binding to a bulky protein partner causes polarisation of the fluorescent emission, which can be detected by a spectrophotometer. Fluorescence polarisation assay was performed using GST-PSD-95 PDZ2 fusion protein and a 12-amino acid FITC-tagged peptide representing the PDZ-BD of PTEN. The standard binding curve was between GST-PSD-95 PDZ2 and PTEN PDZ-BD peptide with an EC₅₀ around 18.26 μM . In contrast, the GST-PSD-95 PDZ1 domain has 30 times less binding capacity. We then tested the reference compound ZL006 at two concentrations at 25 and 50 μM with binding almost completely abolished at 50 μM . We constructed an inhibition curve for ZL006 and yielded an IC₅₀ of 11.76 μM . Screening of 60 ChemDiv compounds identified four small molecules that possessed inhibitory activities but they were not pursued due to their weak inhibitory

effects and undesirable toxicity in animals.

There was no toxicity in mice after administering ZL006 of up to 300 mg/kg. Owing to the potency of the inhibitory activity and apparent lack of toxicity, we decided to focus on ZL006 instead and performed a pull-down assay in mammalian cells. With the addition of ZL006, the interaction between full-length PTEN and GST-PSD-95 PDZ2 was largely suppressed in a dosage-dependent manner.

The Morris water maze test was performed to examine whether ZL006 has therapeutic effects on memory deficits in 5XFAD mice. Two groups of 5XFAD mice were treated with ZL006 (intraperitoneal, 10 mg/kg) for 30 minutes and 2 hours separately before the Morris water maze tests, with the treatment started from day 1 of the training session. Apart from the vehicle control, we treated one group of wild-type mice with ZL006 (intraperitoneal, 10 mg/kg) 2 hours before the tests to determine its effects on normal mice. In the pre-training day, there was no difference in visual and motor ability among the five experimental groups. During the training session, with the administration of ZL006, the five groups showed comparable velocity without significant differences indicating that ZL006 did not alter the motor functions in both wild-type and 5XFAD mice. Importantly, ZL006-treated 5XFAD mice showed shorter escape latency and path length on days 3 and 4 of the training session when compared to the vehicle-treated 5XFAD mice. The effect of ZL006 was evident as early as day 1 as demonstrated by the reduced escape latency. On probe trial day 5, mice treated with ZL006 for 2 hours had increased entries into the platform area and shorter latency to their first swim across the platform area. These findings suggest that ZL006 has therapeutic effects on memory deficits in 5XFAD mice.

Discussion

ZL006 was initially developed as a specific blocker targeting the interaction between nNOS and PSD-95, which forms under ischaemic condition.⁵ The initial goal was to use ZL006 to lower the excitotoxicity associated with excessive glutamate receptor signalling. However, ZL006 could actually inhibit the binding between PTEN PDZ-BD and PSD-95 PDZ2 in fluorescence polarisation and in pull-down assays. We therefore concluded that ZL006 might be a potential compound for treating AD by disrupting the interaction between PTEN and PSD-95. ZL006 may restore synaptic plasticity by promoting LTP or suppressing LTD, or both. There was a lack of major adverse effects of ZL006 based on our toxicity test. We conclude that ZL006 may be effective in restoring normal synaptic transmission to neurons exposed to pathogenic A β at the early phase of AD.

Acknowledgements

The authors acknowledge Prof Wan Chi Cheong in conducting the *in silico* docking analysis, the staff at the Laboratory Animal Services Centre and the Animal Holding Core of the School of Biomedical Sciences of the Chinese University of Hong Kong, and Dr Xian Yanfang and Dr Anthony Chan Siu Lung for preparing the herbal extracts.

Funding

This study was supported by the Health and Medical Research Fund, Food and Health Bureau, Hong Kong SAR Government (#02130026). The full report is available from the Health and Medical Research Fund website (<https://rfs1.fhb.gov.hk/index.html>).

References

1. Shankar GM, Li S, Mehta TH, et al. Amyloid-beta protein dimers isolated directly from Alzheimer's brains impair synaptic plasticity and memory. *Nat Med* 2008;14:837-42.
2. Zhang XC, Piccini A, Myers MP, Van Aelst L, Tonks NK. Functional analysis of the protein phosphatase activity of PTEN. *Biochem J* 2012;444:457-64.
3. Jurado S, Benoist M, Lario A, Knafo S, Petrok CN, Esteban JA. PTEN is recruited to the postsynaptic terminal for NMDA receptor-dependent long-term depression. *EMBO J* 2010;29:2827-40.
4. Knafo S, Sanchez-Puelles C, Palomer E, et al. PTEN recruitment controls synaptic and cognitive function in Alzheimer's models. *Nat Neurosci* 2016;19:443-53.
5. Zhou L, Li F, Xu HB, et al. Treatment of cerebral ischemia by disrupting ischemia-induced interaction of nNOS with PSD-95. *Nat Med* 2010;16:1439-43.

Stochastic stimulation of the motor cortex for treating parkinsonian symptoms: abridged secondary publication

WH Yung *, VCT Mok, Y Ke

KEY MESSAGES

1. Stochastic microcurrent stimulation of the motor cortex could ameliorate parkinsonian motor symptoms in the rodent model.
2. The prototype of the cortical stimulator capable of delivering randomised microcurrents was designed and successfully constructed.
3. Refinement in the density of the microelectrodes is expected to improve the efficacy and robustness of the system.

4. The technology has potential in clinical practice in the future.

Hong Kong Med J 2020;26(Suppl 7):S23-5

HMRF project number: 02130976

¹WH Yung, ²VCT Mok, ¹Y Ke

The Chinese University of Hong Kong:

¹ School of Biomedical Sciences

² Department of Medicine and Therapeutics

* Principal applicant and corresponding author: whyung@cuhk.edu.hk

Introduction

Parkinson disease is a degenerative disorder of the central nervous system mainly affecting the motor system. It is characterised by movement-related symptoms including resting tremor, rigidity, slowness of movement, and difficulty with walking and gait. Parkinson disease is more common in the older population, and the onset usually occurs after the age of 50 years. In Hong Kong, the number of patients with Parkinson disease is estimated to be more than 10 000.¹ As life expectancy continues to increase, the prevalence of Parkinson disease is projected to surge in the coming decades, resulting in an increase of financial and manpower burden to the healthcare system. To date, there is no known cure for Parkinson disease, but some treatments can reduce neural degeneration in the brain and provide relief from motor-related symptoms. Deep brain stimulation (DBS) involves implantation of stimulating electrode that sends electrical pulses targeting at deep brain structures such as the subthalamic nucleus. DBS is considered an effective neurosurgical procedure in reducing motor symptoms, especially in patients receiving maximum pharmacological treatment.² DBS relies on a highly invasive deep brain surgery that sometimes results in infection or intracranial haemorrhage. DBS needs to be guided by intraoperative magnetic resonance imaging for direct visualisation of brain tissue and device, and slightly inaccurate placement of the stimulating electrodes may lead to stimulation of non-target areas and therefore undesirable motor and non-motor adverse effects. Based on our previous findings in experimental animals that DBS could result in the generation of antidromic spikes in the motor cortex,^{3,4} we aim to develop a prototype

of a multi-electrode stimulating array system capable of delivering controlled microcurrents that are randomised in frequency, amplitude, and pulse width to mimic the antidromic spikes arriving at the motor cortex. We also assessed the therapeutic effect of the stochastic cortical stimulation in ameliorating motor symptoms in a rat parkinsonian model.

Methods

Methods used included: construction of custom-design of the cortical stimulation system, generation of a parkinsonian rat model, implantation procedure of stimulation assembly, and assessment of open-field motor behaviour.

Results

Construction of custom-designed cortical stimulator prototype

We constructed a cortical stimulator capable of delivering controlled microcurrents via 16 independent microelectrodes. The main components include microelectrode array, connecting wire, controller board and software control (Fig. 1).

Stimulus parameters that produced uncontrolled motor activities

In the first stage of experimentation, we identified the set of stimulus parameters that would result in undesirable adverse effects on the tested animals. The Table shows some typical combinations of stimuli parameters tested in parkinsonian animals. Some combination of stimulus parameters could result in the generation of uncontrolled seizure-like activity in over 50% of the animals. Examination of the parameters showed that although there was not

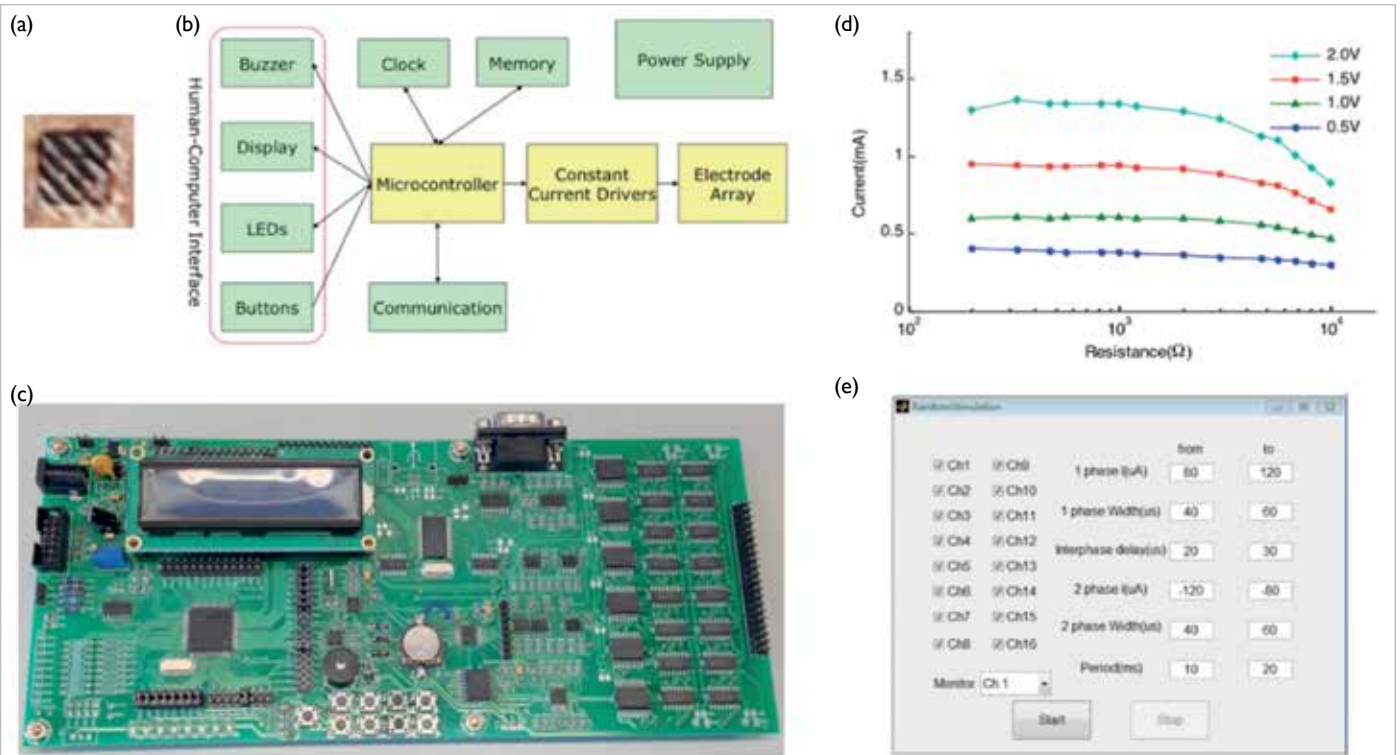
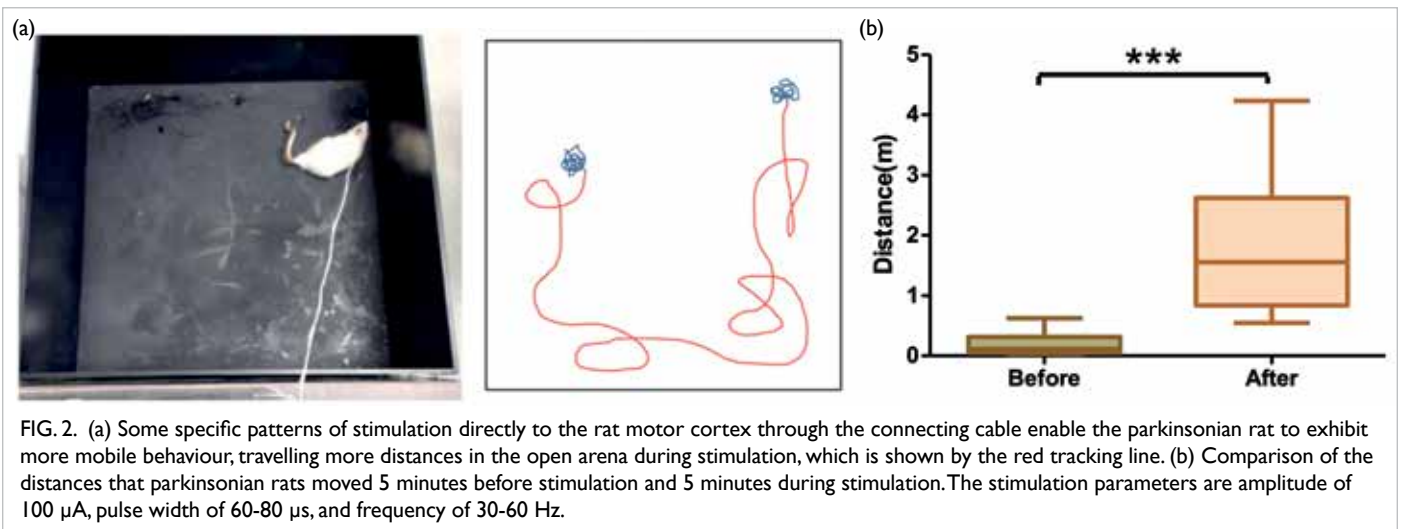


FIG. 1. Prototype of cortical stimulator and controller: (a) The custom-designed and fabricated microelectrode array, (b) the block diagram of the custom-built cortical stimulation controller, (c) the printed circuit board with a 16-channel constant current driver outputting microcurrents to the electrode array, (d) the output performance of the constant current driver at different levels of control voltage, (e) a screenshot of the MATLAB program that sets the location, amplitude, frequency, and pulse width of the randomised microcurrents.

TABLE. Higher values of stimulus parameters can evoke undesirable adverse effects: the highlighted cells are patterns that caused seizures in the Parkinson rat model.

Pulse width, μ s	Frequency of the pulse, Hz	Amplitude of the pulse, μ A	Pulse width, μ s	Frequency of the pulse, Hz	Amplitude of the pulse, μ A	Pulse width, μ s	Frequency of the pulse, Hz	Amplitude of the pulse, μ A	Pulse width, μ s	Frequency of the pulse, Hz	Amplitude of the pulse, μ A	Pulse width, μ s	Frequency of the pulse, Hz	Amplitude of the pulse, μ A
30-60	1-30	100-200	60-90	1-30	100-200	90-120	1-30	100-200	120-150	1-30	100-200	150-180	1-30	100-200
30-60	1-30	200-300	60-90	1-30	200-300	90-120	1-30	200-300	120-150	1-30	200-300	150-180	1-30	200-300
30-60	1-30	300-400	60-90	1-30	300-400	90-120	1-30	300-400	120-150	1-30	300-400	150-180	1-30	300-400
30-60	1-30	400-500	60-90	1-30	400-500	90-120	1-30	400-500	120-150	1-30	400-500	150-180	1-30	400-500
30-60	30-60	100-200	60-90	30-60	100-200	90-120	30-60	100-200	120-150	30-60	100-200	150-180	30-60	100-200
30-60	30-60	200-300	60-90	30-60	200-300	90-120	30-60	200-300	120-150	30-60	200-300	150-180	30-60	200-300
30-60	30-60	300-400	60-90	30-60	300-400	90-120	30-60	300-400	120-150	30-60	300-400	150-180	30-60	300-400
30-60	30-60	400-500	60-90	30-60	400-500	90-120	30-60	400-500	120-150	30-60	400-500	150-180	30-60	400-500
30-60	60-90	100-200	60-90	60-90	100-200	90-120	60-90	100-200	120-150	60-90	100-200	150-180	60-90	100-200
30-60	60-90	200-300	60-90	60-90	200-300	90-120	60-90	200-300	120-150	60-90	200-300	150-180	60-90	200-300
30-60	60-90	300-400	60-90	60-90	300-400	90-120	60-90	300-400	120-150	60-90	300-400	150-180	60-90	300-400
30-60	60-90	400-500	60-90	60-90	400-500	90-120	60-90	400-500	120-150	60-90	400-500	150-180	60-90	400-500
30-60	90-120	100-200	60-90	90-120	100-200	90-120	90-120	100-200	120-150	90-120	100-200	150-180	90-120	100-200
30-60	90-120	200-300	60-90	90-120	200-300	90-120	90-120	200-300	120-150	90-120	200-300	150-180	90-120	200-300
30-60	90-120	300-400	60-90	90-120	300-400	90-120	90-120	300-400	120-150	90-120	300-400	150-180	90-120	300-400
30-60	90-120	400-500	60-90	90-120	400-500	90-120	90-120	400-500	120-150	90-120	400-500	150-180	90-120	400-500

a definitive threshold value of either the stimulus frequency, width, or amplitude that would result in epileptic-like activity, a combination of higher values of pulse width (>120 μ s) and current amplitude (>300 μ A), rather than stimulation frequency, was more likely to generate the undesirable effect.



Stimulus parameters that ameliorated parkinsonian motor symptoms

Systematically examination of the effects of stimulus parameter combinations on locomotor activity showed that some combinations could improve the mobility of the parkinsonian animals. Confining the stimulus amplitude of the pulse to 100-200 μ A, the optimal patterns were pulse width of 60-80 μ s and frequency of 30-60 Hz as well as pulse width of 60-80 μ s and frequency of 90-120 Hz. Typical examples of the effect of stimulation and statistical evaluation are shown in Fig. 2.

Discussion

Our systematic tests for different combinations of stimulation frequency, pulse width, and amplitude demonstrated that some combinations of these parameters at specific ranges could ameliorate motor immobility of parkinsonian rats. Although the degree of improvement was modest, a significant increase in the distance travelled by the animals was found. Given that stochastic nature of microcurrent delivery aiming to break the pathological synchronised activities of cortical neurons, higher values of current amplitude and pulse width could induce seizures, as too strong stimulation would probably cause excessive excitation of the neurons, regardless of the pattern of stimulation. Although the epileptogenic threshold was not defined by electroencephalographic recordings during stimulation, it was inferred by clear uncontrolled activities of the test subject. Future study should define the epileptogenic threshold by more objective measures such as simultaneous electroencephalographic measurement. It should be pointed out that the optimal effective stimulation

frequency is less than that used by the DBS used clinically (ie, 120 Hz). This finding is consistent with our previous discovery that the actual frequency of antidromic spikes generated in DBS is less than the high frequency delivered (ie, 120 Hz). It is likely that the randomised microcurrents at different locations help break the pathological synchronised firing of motor cortical neurons found in parkinsonism.

In this study, we placed a microelectrode array on the cortical surface, rather than deep in the brain, and therefore less invasive to the brain. Less invasive or non-invasive may be a promising direction for Parkinson disease treatment. If the cortical stimulation has equal or better efficacy than DBS, it may replace DBS. In addition, future studies should address the short-term and long-term effects as well as potential interaction with drugs.

Funding

This study was supported by the Health and Medical Research Fund, Food and Health Bureau, Hong Kong SAR Government (#02130976). The full report is available from the Health and Medical Research Fund website (<https://rfs1.fhb.gov.hk/index.html>).

References

1. Hong Kong Parkinson's Disease Foundation. http://www.hkpdf.org.hk/info_sc.php
2. Okun MS. Deep-brain stimulation for Parkinson's disease. *N Engl J Med* 2012;367:1529-38.
3. Li Q, Ke Y, Chan DC, et al. Therapeutic deep brain stimulation in Parkinsonian rats directly influences motor cortex. *Neuron* 2012;76:1030-41.
4. Li Q, Qian ZM, Arbuthnott GW, Ke Y, Yung WH. Cortical effects of deep brain stimulation: implications for pathogenesis and treatment of Parkinson disease. *JAMA Neurol* 2014;71:100-3.

Neuroprotective effects of oxyresveratrol on 6-hydroxydopamine on medial forebrain bundles in a rat model of Parkinson disease: abridged secondary publication

A Shah, YS Ho, KM Ng, M Wang, C Legido-Quigley, RCC Chang *

KEY MESSAGES

1. Oxyresveratrol significantly minimises motor deficits examined by apomorphine-induced rotation test, cylinder asymmetric test, and rotarod test.
2. However, oxyresveratrol cannot significantly reduce the loss of dopaminergic neurons. This suggests that oxyresveratrol per se may not be sufficient to elicit full protection.

Hong Kong Med J 2020;26(Suppl 7):S26-8

HMRP project number: 02131496

^{1,2} A Shah, ³ YS Ho, ⁴ KM Ng, ⁵ M Wang, ^{2,6} C Legido-Quigley, ^{1,7} RCC Chang

¹ Laboratory of Neurodegenerative Diseases, School of Biomedical Sciences, LKS Faculty of Medicine, The University of Hong Kong

² Institute of Pharmaceutical Science, Faculty of Life Sciences and Medicine, King's College London, UK

³ School of Nursing, Faculty of Health and Social Sciences, Hong Kong Polytechnic University

⁴ Department of Chemistry, Faculty of Sciences, The University of Hong Kong

⁵ School of Biological Sciences, Faculty of Sciences, The University of Hong Kong

⁶ Steno Diabetes Center Copenhagen, Gentofte, Denmark

⁷ State Key Laboratory of Brain and Cognitive Sciences, The University of Hong Kong

* Principal applicant and corresponding author: rccchang@hku.hk

Introduction

Nutraceuticals or natural products play protective roles in different neurodegenerative diseases, partly because of their antioxidant properties. These products exhibit prophylactic properties to prevent and delay disease progression. Resveratrol, curcumin, coenzyme Q10, vitamin E, and alpha-lipoate have protective effects in Parkinson disease (PD), but there are no detailed studies about their permeability of the blood-brain barrier (BBB). Therapies for neurodegenerative disease should ideally have high BBB permeability for optimal effects. Oxyresveratrol (OXY) has an enhanced ability to cross the BBB in an in vivo model.¹ OXY is a hydroxyl derivative of resveratrol (RES). It is a stilbene isolated by the hydrolytic activation of Mulberroside A, a compound found primarily in the root of *Morus Alba* (white mulberry). OXY can provide neuroprotective effects against β -amyloid peptide in cultured cortical neurons and hippocampal neurons after cerebral ischaemia by middle cerebral occlusion. OXY can protect neurons from an in vitro traumatic injury model and H₂O₂-induced PC12 cell death. There are enhanced antioxidant effects of OXY over RES. We have shown the neuroprotective effects of OXY on reducing apoptosis in the SH-SY5Y cell line in a PD model.

PD is characterised as the progressive degeneration of a selective group of dopaminergic

(DA) neurons in the substantia nigra pars compacta. Its incidence rate is markedly increased with age, with symptoms including tremor, rigidity, and problems with voluntary movement. Parkinsonian mimetics such as 1-methyl-4-phenylpyridinium and 6-hydroxydopamine (6-OHDA) provide valuable experimental models and preclinical platforms to investigate neuroprotective drugs from nutraceuticals and natural products. We aimed to use a 6-OHDA animal model to investigate the effects of OXY on motor deficits and the neuronal loss of dopaminergic neurons.

Common sites for intracerebral injection of 6-OHDA are the striatum, substantia nigra pars compacta, or the median forebrain bundle (MFB)—the bundle of afferent nerve fibres projecting from the substantia nigra pars compacta to the striatum. In PD, dopaminergic loss is seen in the substantia nigra pars compacta, which results in a 70% to 80% loss of striatal dopamine by the time symptoms are visible. The MFB is the most widely used site for injection, wherein owing to anterograde and retrograde transport, the toxin degenerates both nigral and striatal dopaminergic neurons. Furthermore, cognitive deficits such as spatial memory deficit and mnemonic memory impairment are seen with the MFB model. Thus, the MFB model is a holistic representative of PD and a commonly used model.

Methods

Stereotactic injection of 6-OHDA in an animal model

Male Sprague-Dawley rats aged 4 to 6 weeks weighing 200 g were purchased from the Laboratory Animal Unit at The University of Hong Kong. All experimental procedures were in accordance with the Committee on the Use of Live Animals in Teaching and Research of The University of Hong Kong. Animals of same treatment groups were held in pairs in cages, in a temperature-controlled room with 12 hours dark/light cycles and access to food and water ad-libitum. OXY and RES were dissolved in deionised water to make stock solutions of 1 mg/mL. Rats in the sham or 6-OHDA groups received 1, 10, or 20 mg/kg OXY, 1 or 10 mg/kg RES, or vehicle treatment. Fresh 1 mg/mL stocks of OXY and RES were prepared in water every day, and vortexed until dissolved. Drug was administered by oral gavage at the same time (12:00-14:00) every day. Rats were randomly divided into sham or 6-OHDA group, and received OXY, RES, or vehicle treatment for 1 week before unilateral stereotactic injection of 6-OHDA to induce parkinsonism (on day 8, shortly after oral gavage of drugs on that day). Fresh stock solution (3 µg/µL) of 6-OHDA hydrobromide was prepared in saline (0.9% w/v NaCl) containing 0.2 mg/mL ascorbic acid. The rats were anaesthetised with 60 mg/kg pentobarbital. 12 µg (in 4 µL) of 6-OHDA or vehicle was injected into the right MFB at the rate of 1 µL/minute using a Hamilton syringe. The coordinates for injection were selected as mediolateral (-1.2, from the Bregma), anteroposterior (-4, from the Bregma), and dorsoventral (+7.5, from the dura), with the nose bar position at 4.5, based on the atlas by Paxinos and Watson. Sham animals were injected with the same volume (4 µL) of saline as vehicle. The needle was left in place for 5 minutes before retracting, and the wound was sutured. After suturing, the animals were given meloxicam (dissolved in water) for any pain for 2 days. Rats were allowed to recover, and drug treatment continued for 2 weeks post-surgery.

Animal behavioural tests

At the end of the 3-week treatment, three behaviour tests were carried out to assess intensity of lesion and motor dysfunction as follow:

For asymmetric cylinder test, rats were placed in a transparent acrylic cylinder for 3 minutes and their behaviour recorded. Every time the rat reared, the use of its ipsilateral, contralateral or both forelimbs was counted, for a minimum of three and a maximum of ten rears. The cylinder was cleaned with ethanol between each use. Results were expressed as % trials with ipsilateral use only.

For rotarod test, rats were trained on the rotarod before the start of the entire treatment

plan so as to generate a stable baseline. On the first day of training, rats were first made to walk on the wheel at 5 rotations per minute, to acclimatise to the instrument. Each rat was given three consecutive trials, for three consecutive days. Since the rats had stable latencies to fall by the third day, the average of the three trials on this day was used as the baseline. On the test day (day 22), the rats were given three trials on the wheel again, at the same accelerating speed of 4-40 rotations per minute, over 5 minutes. The latency to fall was noted; and the average of three trials was measured. The results were then expressed as a % decrease of the latency to fall on test day compared to the baseline.

For apomorphine-induced rotation tests, rats were injected subcutaneously with 0.3 mg/kg of apomorphine hydrochloride dissolved in saline. At 5 minutes after injection, each rat was placed in a cylinder and their behaviour recorded for 30 minutes. The number of contralateral rotations in 30 minutes was measured. A contralateral rotation rate of ≥ 4 rotation per minute was considered as acceptable criteria for the model.

Results

Effects of lesions and OXY treatment on body weight

Rats in the 6-OHDA group weighed the least post-surgery, indicating the 6-OHDA unilateral lesion had an effect on body weight. The 6-OHDA + 1 mg/kg OXY rats seemed to show the best recovery in average body weight, whereas the sham + 1 mg/kg showed the highest average body weights among all groups.

Effects of different doses of OXY on the intensity of ipsilateral lesions

At the first stage of treatment, three doses (1, 10, and 20 mg/kg) of OXY were chosen for initial screening. The rats were randomly divided into treatment groups and administered with respective doses of OXY by oral gavage every day, for 1 week before unilateral injection of 6-OHDA. Following surgery (on day 8), OXY treatment continued daily for 2 more weeks. The effects of drug treatment on the intensity of lesion were measured on day 22 using the apomorphine induced rotation test.

After apomorphine (0.3 mg/kg) administration, rats in the 6-OHDA group had a significantly higher number of contralateral rotations in 30 minutes when compared to the sham and sham + drug groups. 10 mg/kg OXY treatment significantly reduced the number of rotations, whereas 1 mg/kg OXY showed a tendency to decrease the number of rotations. The intensity of ipsilateral lesion was thus lowered by drug treatment. Interestingly, 20 mg/kg OXY was not effective in decreasing the number of rotations.

Effects of OXY versus RES on motor function and lesions

Rigidity of the contralateral forelimb induced by unilateral injection of 6-OHDA is a hallmark symptom of PD. An inability to use the contralateral limb and a decreased latency to fall off the rotating wheel were assessed using the cylinder asymmetric test and rotarod tests, respectively. The 6-OHDA-lesioned group showed a higher tendency to use the ipsilateral limb only while rearing, and a significantly lower latency to fall off the rotating wheel, owing to motor imbalance. However, 1 or 10 mg/kg OXY significantly reversed these results. Lesioned animals fed with 1 mg/kg OXY showed a better ability to use their contralateral limbs compared with the 6-OHDA alone group. The 10 mg/kg OXY treated animals also had a higher latency to fall off the rotarod, compared with the 6-OHDA group. The RES-treated groups did not show enhanced motor function like the OXY groups. Unlike 1 or 10 mg/kg OXY, respective doses of RES were not as effective in reducing the number of contralateral rotations. Although 1 mg/kg RES did significantly reduce the percentage of ipsilateral forelimb use, none of the doses of RES was effective in reducing the latency to fall off the rotarod, or the intensity of the lesion, as seen by the apomorphine-induced rotation test.

Discussion

In this study, we established the model validity and the safe dosage range of OXY. Lower doses of OXY (≤ 10 mg/kg) were more effective in reducing the extent of 6-OHDA lesion and motor dysfunction, whereas 20 mg/kg OXY showed little or no effects. In contrast, RES has effect on reduction in motor dysfunction at higher doses in a striatal model of 6-OHDA.^{2,3} In this study, RES was not as effective as OXY at 1 mg/kg or 10 mg/kg. The beneficial effects of RES in an MFB model have not been elucidated. Because the striatal model is less severe than the MFB model, RES might be able to reduce cell damage and loss of motor function in the striatal model. This could explain why all three doses of RES (10, 20, and 40 mg/kg) were still effective in mitigating motor dysfunction.² In summary, we showed that OXY can be used at lower doses up to a certain range. Nonetheless, large-scale studies are warranted to determine the dosage range before any clinical studies assessing the effects of OXY on PD.

Although both 1 and 10 mg/kg OXY showed improvement in motor function, 1 mg/kg OXY did not significantly increase the latency to fall off the rotarod. This dose was however beneficial in alleviating the intensity of the lesion as well as dependence on the ipsilateral forelimb. One reason for discrepancy in these two behavioural tests was body weight. The high average body weights in

1 mg/kg OXY group might interfere with their ability to stay on the rotarod. A significant drop in weight in animals bilaterally lesioned with 6-OHDA was attributed to reduced appetite and motivation.⁴ A certain extent of these effects might also be seen in a unilateral model, affecting their appetite. A study has shown anhedonia and neurotransmitter changes leading to depression initiated by the unilateral 6-OHDA lesion of the MFB.⁵ Anhedonia could also affect on the appetite of animals. A gradual but constant increase in weight of the 6-OHDA + 1 mg/kg OXY-treated animals may indicate that OXY treatment could also reduce psychological changes induced by 6-OHDA, which affect inclination for food.

Taken together, OXY was more potent than RES in facilitating improvement of motor function. A protective agent like OXY seems to be suitable to combat neurodegeneration. Beneficial effects of OXY against PD should be further explored in clinical studies.

Funding

This study was supported by the Health and Medical Research Fund, Food and Health Bureau, Hong Kong SAR Government (#02131496). The full report is available from the Health and Medical Research Fund website (<https://rfs1.fhb.gov.hk/index.html>).

Disclosure

The results of this research have been previously published in:

1. Shah A, Han P, Wong MY, Chang RC, Legido-Quigley C. Palmitate and stearate are increased in the plasma in a 6-OHDA model of Parkinson's disease. *Metabolites* 2019;9:31.

References

- Breuer C, Wolf G, Andrabi SA, Lorenz P, Horn TF. Blood-brain barrier permeability to the neuroprotectant oxyresveratrol. *Neurosci Lett* 2006;393:113-8.
- Jin F, Wu Q, Lu YF, Gong QH, Shi JS. Neuroprotective effect of resveratrol on 6-OHDA-induced Parkinson's disease in rats. *Eur J Pharmacol* 2008;600:78-82.
- Khan MM, Ahmad A, Ishrat T, et al. Resveratrol attenuates 6-hydroxydopamine-induced oxidative damage and dopamine depletion in rat model of Parkinson's disease. *Brain Res* 2010;1328:139-51.
- Ferro MM, Bellissimo MI, Anselmo-Franci JA, Angellucci ME, Canteras NS, Da Cunha C. Comparison of bilaterally 6-OHDA- and MPTP-lesioned rats as models of the early phase of Parkinson's disease: histological, neurochemical, motor and memory alterations. *J Neurosci Methods* 2005;148:78-87.
- Kamińska K, Lenda T, Konieczny J, Czarnecka A, Lorenc-Koci E. Depressive-like neurochemical and behavioral markers of Parkinson's disease after 6-OHDA administered unilaterally to the rat medial forebrain bundle. *Pharmacol Rep* 2017;69:985-94.

Small molecule of adiponectin receptor agonist— AdipoRon—for Alzheimer disease: abridged secondary publication

RCL Ng *, M Jian, M Bunting, SK Chung, KH Chan

KEY MESSAGES

1. Chronic oral administration of AdipoRon reverses spatial learning and memory performance in an Alzheimer mouse model.
2. AdipoRon crosses the blood-brain barrier and reaches maximum concentration 2 hours after oral administration.
3. AdipoRon enhances neuronal insulin sensitivity and reduces amyloid- β deposition.
4. AdipoRon suppresses amyloid- β -mediated neuroinflammatory responses, exerting

protective effects to neurons and synapses in Alzheimer mouse model.

Hong Kong Med J 2020;26(Suppl 7):S29-32

HMRf project number: 03143856

¹RCL Ng, ¹M Jian, ¹M Bunting, ²SK Chung, ¹KH Chan

LKS Faculty of Medicine, The University of Hong Kong:

¹ Department of Medicine

² School of Biomedical Sciences

* Principal applicant and corresponding author: royclng@hku.hk

Introduction

Alzheimer disease (AD) is the most common neurodegenerative cause leading to dementia. The characteristic neuropathological features of AD include amyloid- β -forming neuritic plaques, hyperphosphorylated tau-forming intracellular neurofibrillary tangles, neuroinflammation, and neuronal loss in the hippocampus and frontal cortex. In AD drug invention, immunotherapy-based targeting amyloid- β and tau treatment have demonstrated promising results in mouse models. However, these attempts failed to improve cognitive outcomes in clinical trials. Recently, insulin sensitising and anti-diabetic approaches have provided a new therapeutic strategy to treat AD.

Insulin resistance is a common pathogenesis of both type 2 diabetes mellitus and AD. Diabetic mouse models demonstrated Alzheimer-like alterations and provided evidence that brain insulin resistance is likely to be the main cause of the AD-like pathogenesis.¹ Postmortem AD brains and brains from AD mouse models also showed increased cerebral insulin resistance. Brain insulin resistance increases A β accumulation and tau hyperphosphorylation. Therefore, strategy enhancing insulin sensitivity becomes a promising therapeutic method to treat AD.

Adiponectin is an insulin-sensitising adipokine with anti-inflammatory and anti-oxidative effects. Hypoadiponectinaemia is a risk factor of insulin resistance-associated type 2 diabetes mellitus. Findings are inconclusive in whether high or low level of adiponectin is associated with AD. We have revealed that chronic adiponectin deficiency results

in AD-like pathologies and cognitive impairments in aged mice, and these mice develop cerebral insulin resistance with reduced hippocampal insulin sensitivity.² AdipoRon is a newly invented adiponectin receptor agonist that can be orally administered. It can improve glucose uptake, lipid metabolism, and insulin sensitivity in mammalian cells and in mice. Life span has been increased in high-fat-diet-fed *db/db* mice (an animal model for type 2 diabetes mellitus and obesity) through metabolic improvement after oral administering AdipoRon. Therefore, we hypothesise that AdipoRon can be a promising therapeutic drug for AD by enhancing insulin sensitivity and suppressing neuroinflammation. In this project, we demonstrated that oral administration of AdipoRon reversed cognitive deficits in transgenic AD mice. AdipoRon-treated AD mice showed increased neuronal insulin sensitisation, ameliorated neuropathologies, and reduced neuroinflammatory responses.

Methods

To determine if AdipoRon is a blood-brain barrier penetrant, pharmacokinetics of AdipoRon in mice plasma and the brain were determined quantitatively. C57BL6/N mice (20–25 g) were randomly divided into seven groups with three mice in each group. Each mouse was orally administered 50 mg/kg AdipoRon dissolved in corn oil. The mice were euthanised at 0, 0.5, 1, 2, 4, 8, or 12 hours after drug administration, and blood and brain tissue were collected. Plasma samples were obtained by centrifuging the blood at 3500 \times g for 5 minutes, and brain tissue was homogenised and processed to extract the content.

Finally, 10 μ L of the reconstituted solution was analysed by LC-MS/MS. The concentrations of AdipoRon in different samples were determined by coupled to an API3200 triple quadrupole MS (Sciex, Ontario, Canada) that was equipped with a TurboIonSpray ion source.

Five-month-old 5xFAD mice were fed with AdipoRon (50 mg/kg bodyweight) by oral gavage daily. Littermate controls were fed with vehicle. After 3 months of administration, mice were subjected to behavioural analysis including Morris water maze test for their spatial learning and memory functions, open field test for anxiety level, and fear-conditioning test for hippocampal-dependent memory of aversive stimuli. >10 animals underwent these behavioural tests.

To determine whether AdipoRon treatment enhances insulin signalling activities, the hippocampus was dissected and was snap-frozen for western blot analysis of insulin signalling molecules. Hippocampal insulin sensitivity was also examined by injecting recombinant insulin to the right hippocampus with or without AdipoRon administration using stereotaxic instruments. Induction of insulin signalling in the hippocampus was determined by western blot analysis.

Neuropathological changes, in the control and AdipoRon-treated AD mice, including amyloid- β deposition, microgliosis, astroglia, and neuronal loss were examined by immunofluorescent staining using corresponding primary antibodies. Golgi-Cox staining was performed to visualise the spine density of the hippocampal apical dendrites.

Statistical analyses were performed with GraphPad Prism 6 (GraphPad Software). For the Morris water maze test, dataset was analysed by two-way ANOVA. Other behavioural tests were analysed by one-way ANOVA. In other experiments, between-group differences were determined with one-way ANOVA, followed by Bonferroni post hoc test. Alternatively, the mean significant difference between two groups was determined with two-tailed unpaired Student's *t*-test. Statistical significance was defined as $P < 0.05$.

Results

AdipoRon crosses the blood-brain barrier and increases AMPK phosphorylation

The pharmacokinetics of AdipoRon in the plasma and the brain were studied by LC-MS/MS analysis. Plasma AdipoRon reached the maximum level 2 hours after oral gavage. AdipoRon was detected in the brain samples, with the highest level at 2 hours after oral gavage. This provides concrete evidence that AdipoRon can cross the blood-brain barrier. We then investigated if AdipoRon activated adiponectin signalling by increasing AMPK phosphorylation in the hippocampal lysates. Western blot analysis

indicated that the pAMPK levels of the hippocampus were increased 2 hours after AdipoRon treatment compared to the vehicle treatment.

AdipoRon reverses memory and cognitive functions

To investigate if chronic AdipoRon administration can improve cognitive and memory functions of AD mouse model, 5xFAD mice at age 5.5 months were fed with AdipoRon daily by oral gavage for 3 months. The mice were then examined with the anxiety levels by open field test, in which less time spent at the centre indicates higher anxiety level for the mice. Interestingly, AdipoRon-treated mice spent significantly increased time than vehicle-treated mice. This result showed that AdipoRon reduced anxiety levels in the AD mouse model.

To assess the learning and memory functions, the Morris water maze test was performed. Analysis confirmed an overall learning and memory impairment in 9-month-old 5xFAD mice compared to wildtype mice. 5xFAD with chronic AdipoRon treatment reversed the overall learning and memory performance with shorter escape latency after 5 days of the hidden test. Furthermore, the probe test revealed AdipoRon-treated 5xFAD mice spent more time in the target quadrant compared with the vehicle-treated littermates.

AdipoRon treatment significantly improved the performance of 5xFAD mice in the contextual fear conditioning tests compared with the vehicle-treated littermates. However, we did not observe improvement in the freezing response in the cued fear conditioning tasks. All these results indicate that AdipoRon improved hippocampus-dependent learning and memory functions in the AD mouse model.

AdipoRon enhances neuronal and cerebral insulin sensitisation

AdipoRon markedly increased the levels of Akt phosphorylation at serine 473 residue and GSK3 β at serine 9 residue, comparable to the levels of wildtype mice. On the contrary, the phosphorylation of IRS-1 at serine 616, which related to insulin resistance, was reduced in the AdipoRon-treated 5xFAD mice. In the stereotaxic injection experiment, vehicle-treated 5xFAD showed insignificant increased of pAkt^{S473} levels, whereas AdipoRon-treated 5xFAD mice showed a significant increase in the level of pAkt^{S473}. These data show that aberrant reduction of insulin signalling in 5xFAD mice was enhanced after oral administration of AdipoRon.

AdipoRon reduces amyloid pathology and neuroinflammation

To examine the effect of AdipoRon on amyloid- β deposition in the brain, we observed the levels

of amyloid- β plaques in mice subjected to the behavioural studies. Brain sections were stained with thioflavin S (ThioS) to visualise insoluble β -sheet amyloid- β deposits. Total number and amyloid- β loading found in the cerebral cortex and hippocampus were quantified. The amyloid- β loading and number of deposits was dramatically reduced in these brain regions of AdipoRon-administered 5xFAD mice compared with vehicle controls.

To investigate if AdipoRon reduced microgliosis and astrogliosis, the brain sections were immunostained with Iba1 (microglia marker) and GFAP (astrocyte marker). Our results indicated that both Iba1 and GFAP levels were reduced in the cerebral cortex and hippocampus of AdipoRon-treated 5xFAD mice compared with that of vehicle-treated 5xFAD mice. We also studied the levels of proinflammatory cytokines (IL1 β and TNF α) by ELISA analysis. These cytokines have demonstrated detrimental effects on neurons in AD brains. The levels of IL1 β and TNF α increased in the brains of 5xFAD mice compared with wildtype mice. Importantly, 5xFAD with chronic AdipoRon administration had reduction of IL1 β and TNF α levels. These results demonstrated that AdipoRon reduced neuroinflammatory responses in the transgenic AD model.

AdipoRon restores neuronal loss and dendritic spine reduction

To quantify hippocampal neurons, we performed NeuN immunostaining to visualise CA1 neurons. We found an insignificant decrease of CA1 neurons in the vehicle-treated 5xFAD mice compared to wildtype, whereas AdipoRon-treated mice showed a comparable number of NeuN-stained neurons. Moreover, we examined if the memory improvement after AdipoRon administration associated with neuronal and synaptic changes. We performed double immunofluorescent staining of Ctip2 and Brn2 to label and quantified the layer V neurons in different mice group. 5xFAD mice had reduced layer V cortical neurons compared with wildtype mice. AdipoRon-treated 5xFAD mice had a significant increase of the layer V neurons compared with 5xFAD mice.

In the Golgi-Cox staining, we found an overall decrease in spine density in vehicle-treated 5xFAD mice relative to littermate wildtype. Importantly, AdipoRon-treated 5xFAD mice revealed a complete restoration of the spine deficit in apical dendrites of the CA1 layer.

Discussion

Orally administered adiponectin receptor agonist could cross the blood-brain barrier. Pharmacokinetic study demonstrated that AdipoRon reached the highest concentration in the brain and plasma

simultaneously. However, the half-life of AdipoRon was short. The molecule was almost undetectable by LC-MS/MS 6 hours after oral administration. Therefore, the mice were fed with AdipoRon for 3 months. We provided concrete evidence supporting AdipoRon as a promising medication to treat AD. Long-term AdipoRon administration reduced neuropathologies in AD mice with significant improvement of cognitive and memory functions. However, structure modification of the molecule may be necessary to prolong the half-life of AdipoRon in order to maximise the therapeutic effects.

Apart from insulin sensitising, adiponectin is an anti-inflammatory agent, our results also demonstrated that AdipoRon could suppress neuroinflammatory responses by reducing activation of microglia and astrocyte. Activation of these glial cells is detrimental because the activated glia produces high levels of proinflammatory cytokines. These cytokines are toxic to neuron and can affect neuronal function.³ From our data, cerebral proinflammatory cytokine levels were significantly reduced after AdipoRon administration. This provided an explanation that 5xFAD mice were protected from neuronal and synaptic reduction after treating with AdipoRon.

Reports indicated that adiponectin could promote hippocampal neurogenesis and dendritic spine formation.^{4,5} From our data, AdipoRon prevented neuronal loss and spine reduction. However, it may also increase neurogenesis to increase the number of functional neurons and promotes spine formation. These require further study to investigate if AdipoRon can restore the number of neurons at the late stage of AD.

Conclusion

AdipoRon can reverse memory impairments, reduce anxiety levels, and improve neuropathology in AD mice. AdipoRon enhances neuronal insulin sensitivity and ameliorates insulin resistance in the hippocampus. AdipoRon can also reduce inflammatory responses and cytokines levels. These support the potential therapeutic effects of AdipoRon to treat AD.

Acknowledgements

We thank Prof Min Li of Hong Kong Baptist University for assisting the experiment of fear conditioning test. We also thank Prof Kiren Rockenstein of Salk Institute for sharing the immortalised hippocampal neurons (HT-22).

Funding

This study was supported by the Health and Medical Research Fund, Food and Health Bureau, Hong

Kong SAR Government (#03143856). The full report is available from the Health and Medical Research Fund website (<https://rfs1.fhb.gov.hk/index.html>).

Disclosure

The results of this research have been previously published in:

1. Ng RC, Jian M, Ma OK, et al. Chronic oral administration of adipoRon reverses cognitive impairments and ameliorates neuropathology in an Alzheimer's disease mouse model. *Mol Psychiatry* 2020;10.1038/s41380-020-0701-0.

References

1. de la Monte SM. Brain insulin resistance and deficiency as therapeutic targets in Alzheimer's disease. *Curr Alzheimer*

Res 2012;9:35-66.

2. Ng RC, Cheng OY, Jian M, et al. Chronic adiponectin deficiency leads to Alzheimer's disease-like cognitive impairments and pathologies through AMPK inactivation and cerebral insulin resistance in aged mice. *Mol Neurodegener* 2016;11:71.
3. Floden AM, Combs CK. Beta-amyloid stimulates murine postnatal and adult microglia cultures in a unique manner. *J Neurosci* 2006;26:4644-8.
4. Zhang D, Wang X, Lu XY. Adiponectin exerts neurotrophic effects on dendritic arborization, spinogenesis, and neurogenesis of the dentate gyrus of male mice. *Endocrinology* 2016;157:2853-69.
5. Song J, Kang SM, Kim E, Kim CH, Song HT, Lee JE. Adiponectin receptor-mediated signaling ameliorates cerebral cell damage and regulates the neurogenesis of neural stem cells at high glucose concentrations: an in vivo and in vitro study. *Cell Death Dis* 2015;6:e1844.

Modified Huang-Lian-Jie-Du-Tang and its combination with memantine for Alzheimer disease: an in vivo study (abridged secondary publication)

SSK Durairajan *, M Li, SK Chung, QB Han, A Iyaswamy, SG Sreenivasmurthy, S Malampati, AK Kammala

KEY MESSAGES

1. Huang-Lian-Jie-Du-Tang (HLJDT) is composed of *Rhizoma coptidis*, *Radix scutellariae*, *Cortex phellodendri*, and *Fructus gardenia* at the ratio of 3:2:2:3. It is a famous traditional Chinese medicine. We found that HLJDT increased the amyloid- β (A β) load in an Alzheimer disease mouse model owing to the APP-increasing effect of baicalein, which is the main pure compound of a constituent herb, *Radix scutellariae*.
2. In contrast, the modified HLJDT is composed of *Rhizoma coptidis*, *Cortex phellodendri*, and *Fructus gardenia* in the ratio of 4:2:4, and showed both memory-enhancing effect and A β -reducing effects in an Alzheimer disease mouse model.
3. Upon confirming the modified HLJDT's efficacy

and safety profile in clinical trials, the modified HLJDT may be prescribed for treating Alzheimer disease.

Hong Kong Med J 2020;26(Suppl 7):S33-6

HMRP project number: 11122511

^{1,2} SSK Durairajan, ¹ M Li, ³ SK Chung, ¹ QB Han, ¹ A Iyaswamy, ¹ SG Sreenivasmurthy, ¹ S Malampati, ¹ AK Kammala

¹ School of Chinese Medicine, Hong Kong Baptist University

² Department of Microbiology, School of Life Sciences, Central University of Tamil Nadu, Tiruvarur, India

³ Beijing Normal University-Hong Kong Baptist University, United International College, Zhuhai, Guangdong Province, China

* Principal applicant and corresponding author:
d.sivasundarakumar@cutn.ac.in

Introduction

Alzheimer disease (AD) is a persistently progressing neurodegenerative disorder. One AD pathogenesis is the accumulation of the amyloid- β peptide (A β).¹ We have identified a novel function of modified Huang-Lian-Jie-Du-Tang (HLJDT-M) in treating AD through *in vitro* studies.² In this project, we validated the *in vivo* efficacy of both HLJDT and HLJDT-M in a triple transgenic mouse model of AD (3XTg-AD). We have also investigated the combinational effect of HLJDT-M with anti-AD drug memantine for the clearance of the A β plaques and memory improvement in a mouse model of AD. HLJDT, HLJDT-M, and HLJDT + memantine were used to treat 3XTg-AD mice for 6 months, and the memory retention and decrease in the load of A β plaques were evaluated.

Methods

Memory retention and A β plaque load were assessed by the Morris water maze and immunohistochemical analysis, respectively, as described previously.³ ELISA was used to measure the levels of A β 1-40 and A β 1-42. The underlying mechanism of the clearance of the A β products was explored by Western blotting analysis. Chromatographic and mass spectroscopic techniques were implemented for analysing the qualities of the extracts.

Results

Berberine was the highest content of the active component present in the aqueous extracts of the HLJDT-M, followed by geniposide and palmatine (Fig.1). During Morris water maze, the spatial reference memory significantly enhanced only after prolonged treatment of HLJDT-M, compared with vehicle or HLJDT (Fig. 2). After oral administration of HLJDT-M for 7 months, the travel distance to locate the hidden platform significantly decreased, and the spatial learning tasks significantly improved after 4 to 5 days, compared with no significant improvement in HLJDT- or vehicle-treated 3xTg-AD mice. These results suggest that spatial learning of 3XTg-AD mice was not enhanced in the HLJDT-treated group but was ameliorated in the HLJDT-M-treated group. Combination of HLJDT-M with memantine did not show further improvement in memory.

Immunohistochemical analysis showed that the load of A β plaques was significantly decreased in HLJDT-M-treated mice, compared with the vehicle-treated group, whereas HLJDT treatment further increased the load. These results were also confirmed in ELISA. HLJDT-M-treated mice had significantly reduced soluble levels of A β 1-42 by 29% and insoluble levels of A β 1-42 by 34%. In contrast, the soluble and insoluble levels of A β 1-42 were significantly increased in the HLJDT-treated mice (Fig. 3).

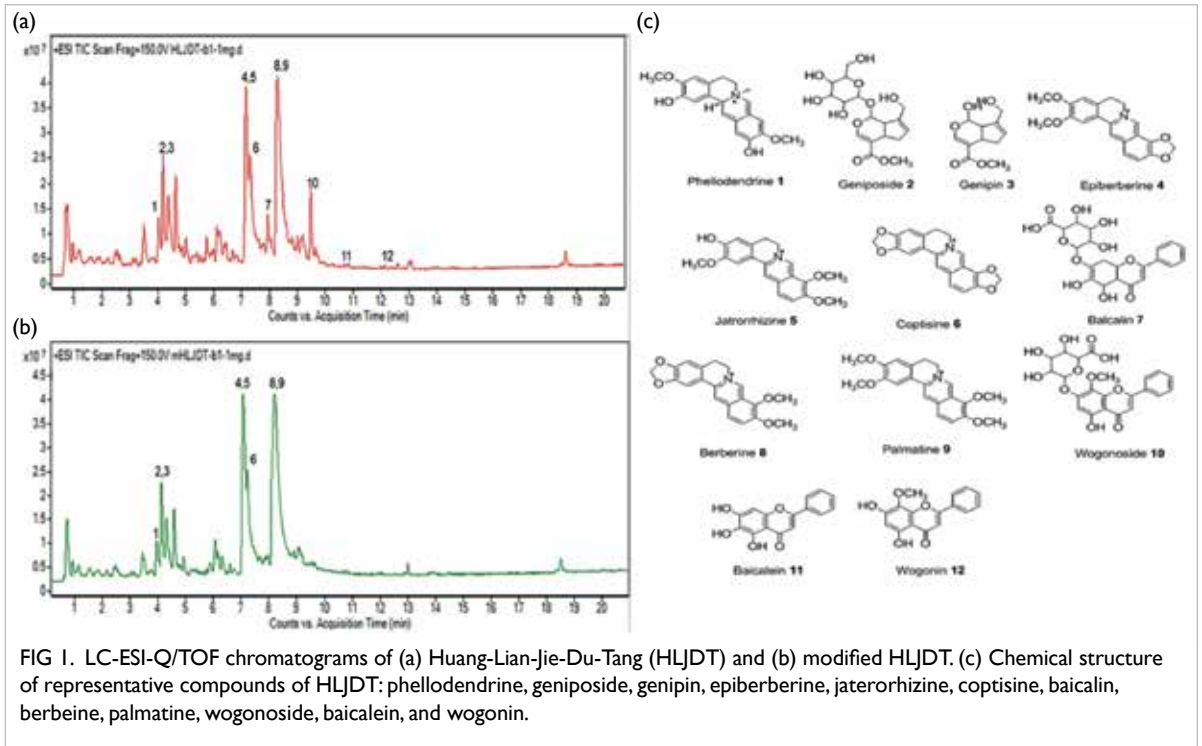


FIG 1. LC-ESI-Q/TOF chromatograms of (a) Huang-Lian-Jie-Du-Tang (HLJDT) and (b) modified HLJDT. (c) Chemical structure of representative compounds of HLJDT: phellodendrine, geniposide, genipin, epiberberine, jatrorrhizine, coptisine, baicalin, berberine, palmatine, wogonoside, baicalein, and wogonin.

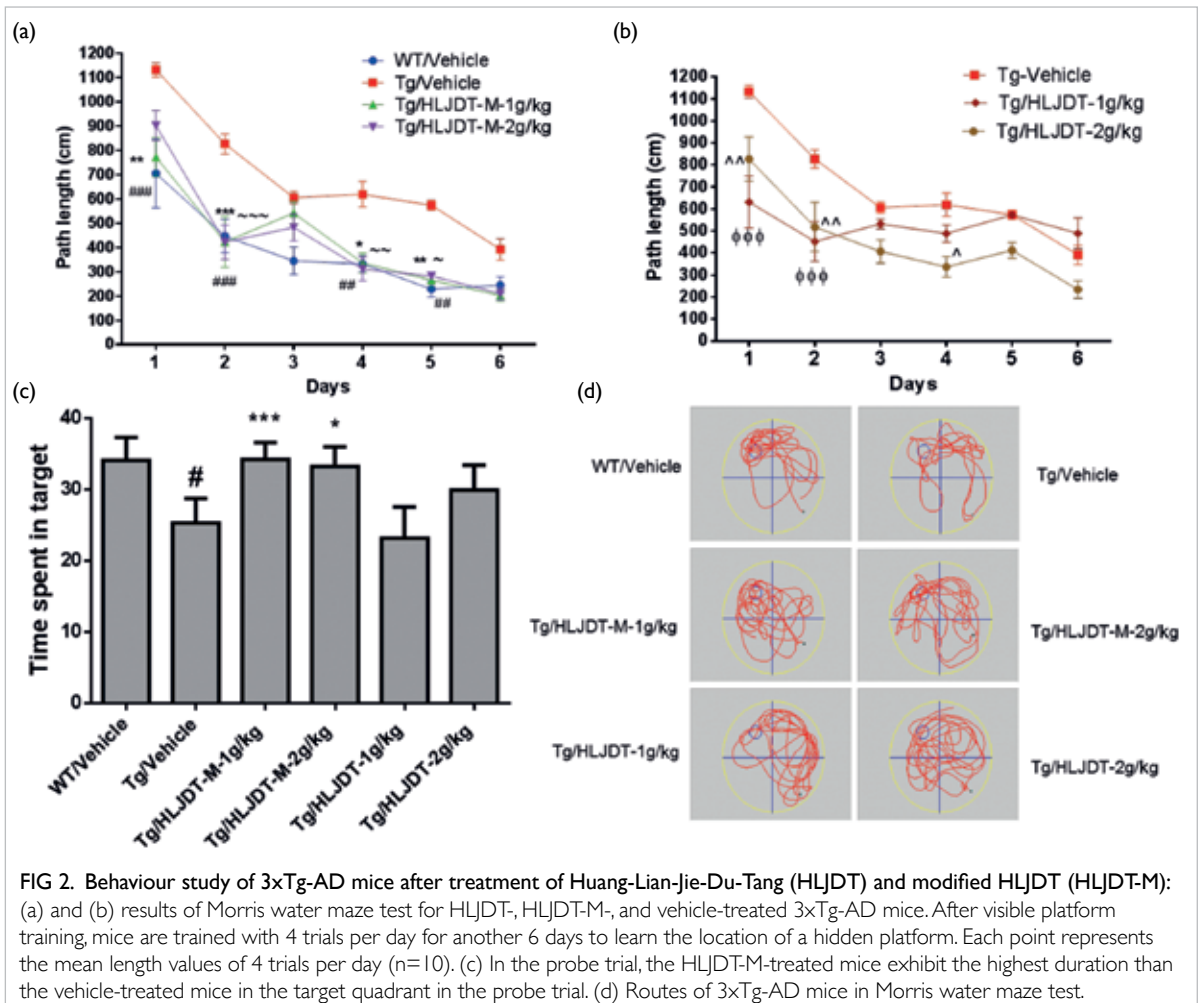


FIG 2. Behaviour study of 3xTg-AD mice after treatment of Huang-Lian-Jie-Du-Tang (HLJDT) and modified HLJDT (HLJDT-M): (a) and (b) results of Morris water maze test for HLJDT, HLJDT-M-, and vehicle-treated 3xTg-AD mice. After visible platform training, mice are trained with 4 trials per day for another 6 days to learn the location of a hidden platform. Each point represents the mean length values of 4 trials per day (n=10). (c) In the probe trial, the HLJDT-M-treated mice exhibit the highest duration than the vehicle-treated mice in the target quadrant in the probe trial. (d) Routes of 3xTg-AD mice in Morris water maze test.

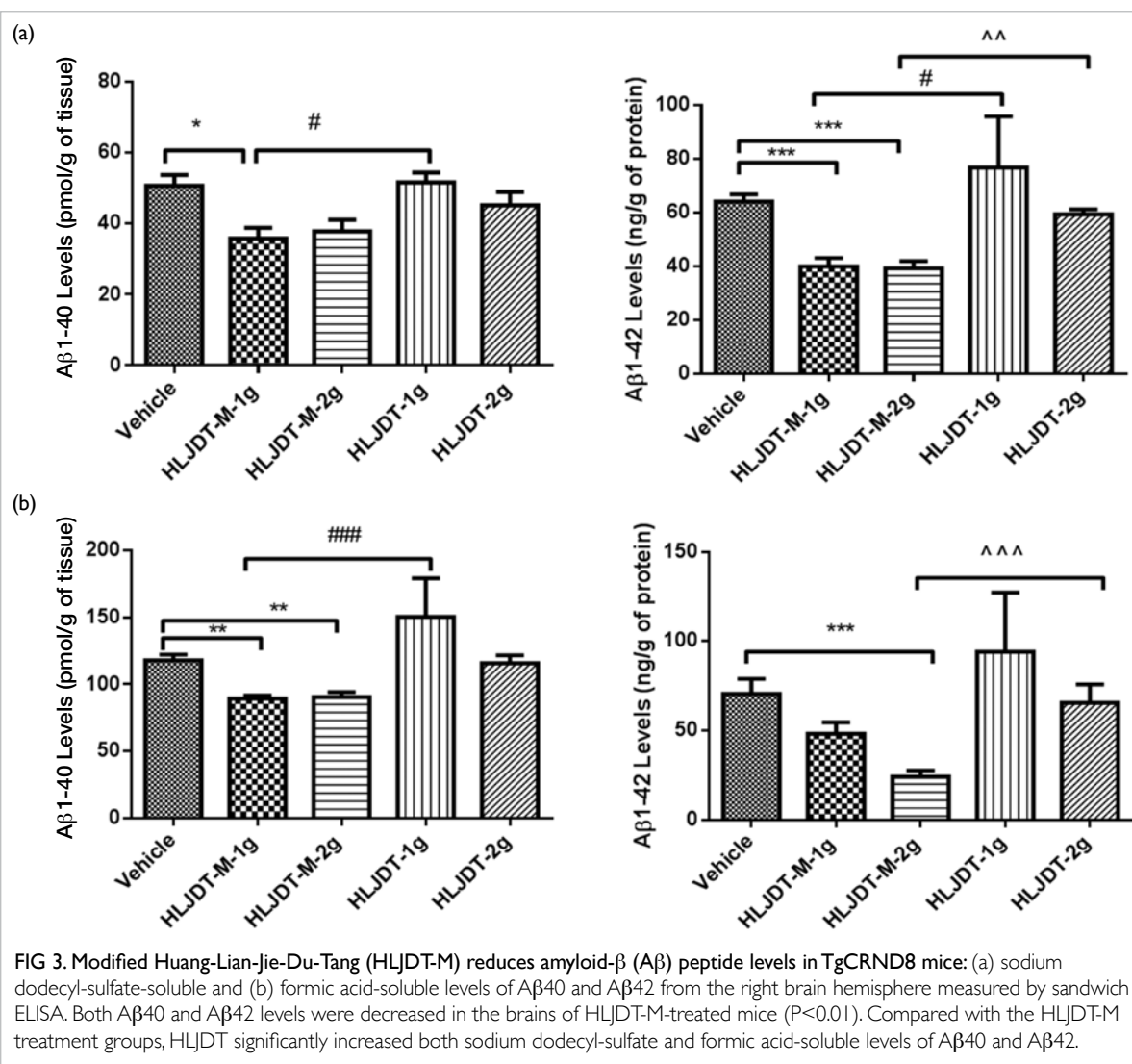


FIG 3. Modified Huang-Lian-Jie-Du-Tang (HLJDT-M) reduces amyloid- β (A β) peptide levels in TgCRND8 mice: (a) sodium dodecyl-sulfate-soluble and (b) formic acid-soluble levels of A β 40 and A β 42 from the right brain hemisphere measured by sandwich ELISA. Both A β 40 and A β 42 levels were decreased in the brains of HLJDT-M-treated mice ($P < 0.01$). Compared with the HLJDT-M treatment groups, HLJDT significantly increased both sodium dodecyl-sulfate and formic acid-soluble levels of A β 40 and A β 42.

To understand the mechanism of A β clearance, the sodium dodecyl-sulfate fraction of brain lysate were analysed for FI-APP, CTFs, and pAPP^{Thr668}. Results from the Western blotting showed that the levels of APP and CTF were significantly decreased after treatment of HLJDT-M. Regarding the levels of pAPP and pCTFs, the decrease was 39% and 50%, respectively, in the 1g/kg of the HLJDT-M treatment group, and was 43% and 44%, respectively, in the 2g/kg of the HLJDT treatment group, compared with vehicle control group. In contrast, all metabolic products of APP significantly were increased to an even greater extent in 1g/kg than 2g/kg of the HLJDT treatment group.

Discussion

HLJDT-M treatment by oral gavage reduced the A β plaque deposition and gliosis, and improved spatial learning and memory retention deficits in 3xTg-AD mice. Further, HLJDT-M treatment significantly decreased all the APP metabolic products including

A β . HLJDT-M has profound effect on the clearance of A β 1-42 and on decreasing the levels of pAPP/pCTFs. These data suggest that HLJDT-M has neuroprotective effects in AD mice via decreasing all metabolites of APP and by improving the memory retention.

Funding

This study was supported by the Health and Medical Research Fund, Food and Health Bureau, Hong Kong SAR Government (#11122511). The full report is available from the Health and Medical Research Fund website (<https://rfs1.fhb.gov.hk/index.html>).

Disclosure

The results of this research have been previously published in:

1. Durairajan SSK, Iyaswamy A, Shetty GS, et al. A modified formulation of Huanglian-Jie-Du-Tang reduces memory impairments and β -amyloid plaques in a triple transgenic mouse model of

Alzheimer's disease. *Sci Rep* 2017;7:6238.

2. Durairajan SS, Huang YY, Yuen PY, et al. Effects of Huanglian-Jie-Du-Tang and its modified formula on the modulation of amyloid- β precursor protein processing in Alzheimer's disease models. *PLoS One* 2014;9:e92954.

References

1. Selkoe DJ. Cell biology of protein misfolding: the examples of Alzheimer's and Parkinson's diseases. *Nat Cell Biol* 2004;6:1054-61.
2. Durairajan SS, Huang YY, Yuen PY, et al. Effects of Huanglian-Jie-Du-Tang and its modified formula on the modulation of amyloid- β precursor protein processing in Alzheimer's disease models. *PLoS One* 2014;9:e92954.
3. Durairajan SS, Liu LF, Lu JH, et al. Berberine ameliorates β -amyloid pathology, gliosis, and cognitive impairment in an Alzheimer's disease transgenic mouse model. *Neurobiol Aging* 2012;33:2903-19.

Lutein for alleviating early high mortality and brain pathology after experimental stroke in a genetic type I diabetic mouse model: abridged secondary publication

AKW Lai, DTC Ng, BKC Tam, FKC Fung, SK Chung, ACY Lo *

KEY MESSAGES

1. Hyperglycaemia plays an important role in the rapid exacerbation of stroke by compromising blood vessel integrity and increasing haemorrhagic transformation, resulting in extensive inflammation and high mortality.
2. These exacerbations are partially contributed by VEGF up-regulation, which has deleterious effects via triggering robust inflammation and vascular hyperpermeability.
3. After 0.5 hour of ischaemia, *Ins2^{Akita/+}* mice displayed a delayed but significant development of infarct.

4. Lutein treatment reduced neurological deficits (after 0.5 hour of ischaemia) and mortality rate (after 2 hours of ischaemia).

5. Lutein is a potential treatment for stroke patients with type 1 diabetes.

Hong Kong Med J 2020;26(Suppl 7):S37-41

HMRP project number: 03142256

¹ AKW Lai, ¹ DTC Ng, ¹ BKC Tam, ¹ FKC Fung, ² SK Chung, ¹ ACY Lo

Li Ka Shing Faculty of Medicine, The University of Hong Kong:

¹ Department of Ophthalmology

² School of Biomedical Sciences

* Principal applicant and corresponding author: amylo@hku.hk

Introduction

The incidence of stroke in patients with type 1 diabetes is four-fold higher than that in the general population. These patients are prone to die from stroke,¹ with shortened median survival² and more haemorrhagic transformation. We aimed to identify the causation of exacerbation of symptoms in patients with diabetes upon stroke using *Ins2^{Akita/+}* mice, a model of type 1 diabetes carrying a point mutation in *Insulin 2 (Ins2)* gene.³ Lutein is an anti-inflammatory and anti-oxidative agent that exerts neuroprotective effects in wildtype mice upon middle cerebral artery occlusion.⁴ We aimed to determine the efficacy of lutein under hyperglycaemic conditions.

Methods

Male *Ins2^{Akita/+}* mice (11-16 weeks old) were used and kept under a 12-hour light/dark cycle with free food and water access. Experiments were approved by the Committee on the Use of Live Animals in Teaching and Research of The University of Hong Kong.

The mice were subjected to transient focal cerebral ischaemia using the intraluminal method.⁴ Animals in sham control groups received the same experimental procedures except for filament insertion. Two hours of ischaemia and the corresponding sham operation were induced in both *Ins2^{+/+}* and *Ins2^{Akita/+}* mice, followed by either 2 or 22 hours of reperfusion (2hI/2hR and 2hI/22hR groups, respectively). 0.5 hour of ischaemia was induced only in *Ins2^{Akita/+}* mice with either 3.5 or 23.5 hours of reperfusion (0.5hI/3.5R and

0.5hI/23.5hR groups, respectively).

In the 2hI/2hR group, lutein (0.2 mg/kg) was administered intraperitoneally twice at 1 hour before and 1 hour after reperfusion. In the 0.5hI/23.5hR group, 2 mg/kg lutein was administered once at 10 minutes before reperfusion. Control mice received the same treatment with 10% DMSO injection (vehicle).

The number of deaths was recorded, and neurological deficits were evaluated at the end of reperfusion using a scoring system.⁴

Brains were isolated and cut into five 2-mm-thick coronal slices using a brain matrix (RBM-2000C, ASI instruments). Brains slices were stained with 2% 2,3,5-triphenyltetrazolium chloride (TTC) at 37°C for 7.5 minutes and fixed in 10% buffered formalin overnight. The red and white regions (live and infarct tissues, respectively) on the posterior side were photographed and measured using Sigma ScanPro. The infarct areas and volume were estimated using an indirect method.⁴ Haemorrhage transformations, as measured by total dark brown areas on the posterior side of TTC-stained brain slice no. 3 (approximately at bregma -0.34 mm), was presented as percentages.

For histological and immunohistochemical analysis, fixed brain slices were paraffin-embedded and sectioned (7 µm). Patches of orange red area after haematoxylin and eosin staining indicated the presence of haemorrhage. The sections were also immune-stained with anti-ZO-1 and anti-MMP-9 antibodies.

For Western blot analysis, brain lysates

were mixed with 2× ice-cold RIPA lysis buffer and analysed using antibodies against β -tubulin, α -actin, matrix metalloproteinase (MMP)-2, MMP-9, ZO-1, vascular endothelial growth factor (VEGF), extracellular signal-regulated kinase (total Erk), p-Erk, p38 mitogen-activated protein kinase (total p-38 MAPK), and p-p38 MAPK. Signals were detected by ECL and quantified using Image J.

For real-time PCR analysis, brain lysates were mixed with ice-cold RNeasy lysis buffer and total RNA was extracted. cDNA was prepared from 2 μ g of extracted RNA. Real-time PCR reactions were performed based on SYBR Green technology using StepOnePlus system for: α -actin, ATF6, BiP, CHOP, pERK, IRE1 α , Atg12, Bcl2, LC3-a, LC3-b, and p62.

Data were expressed as mean \pm standard error of mean or standard error. Survival rate and neurological score were analysed using the log-rank (Mantel-Cox) test and Mann-Whitney *U* test, respectively. All other measurements were analysed using one-way ANOVA, followed by Bonferroni post hoc test or unpaired student's *t*-test. A *P* value of <0.05 was considered statistically significant.

Results

Ins2^{Akita/+} mice showed decreased survival rate, worsen neurological outcomes, accelerated development of infarct, increased haemorrhage, and decreased vessel integrity. Ins2^{Akita/+} mice showed significantly lower survival rate at 2 and 22 hours after reperfusion (Figs. 1a & 1b). Most deaths occurred in the first 4 hours after reperfusion in Ins2^{Akita/+} mice but occurred generally later in Ins2^{+/+} mice. Moreover, Ins2^{Akita/+} mice had a more severe neurological deficit at 2 hours after reperfusion, compared with Ins2^{+/+} mice (Figs. 1c & 1d). At 2 hours after reperfusion, infarct area was significantly larger in brain slice no. 1-3 of Ins2^{Akita/+} brains, compared with Ins2^{+/+} brains. The infarct area robustly exacerbated at 22 hours after reperfusion in Ins2^{Akita/+} brains, compared with Ins2^{+/+} brains (Figs. 1e to 1k).

Western blot analysis at 2 hours after reperfusion revealed that ZO-1 level was significantly reduced, the expression of MMP-9 (a matrix metalloproteinase known to disrupt the blood brain barrier following stroke) was increased (but not significantly), and the expression of MMP-2 was significantly up-regulated in Ins2^{Akita/+} mice, compared with Ins2^{+/+} mice (Fig. 2a). At 2 hours after reperfusion, inflammatory markers VEGF, p-Erk1/2, and p-p38 MAPK were significantly over-expressed in Ins2^{Akita/+} brains, compared with Ins2^{+/+} brains (Fig. 2a). Similarly, at 22 hours after reperfusion, VEGF expression remained significantly increased only in Ins2^{Akita/+} mice (Fig. 2b). Significant increase of p-Erk1/2 expression was found in both Ins2^{+/+} and Ins2^{Akita/+} brains, yet the level in Ins2^{Akita/+} mice was significantly higher. Increased CHOP expression

was also more pronounced in Ins2^{Akita/+} mice at 2 hours after reperfusion.

Compared with vehicle mice, in Ins2^{Akita/+} mice administration of two low doses of lutein (0.2 mg/kg) yielded a lower mortality rate in the 2hI/2hR group and significantly reduced neurological deficits in the 0.5hI/23.5hR group that had the same infarct size but milder neurological deficits (Fig. 3).

Discussion

Induction of ischaemic stroke in hyperglycaemic Ins2^{Akita/+} mice could mimic the exacerbated outcomes similar to those observed in patients with type 1 diabetes upon stroke. Earlier and more robust inflammatory responses and increase in pro-apoptotic CHOP were potentially responsible for the aggravation.

Haemorrhagic transformation was observed in Ins2^{Akita/+} mice at 2 hours after reperfusion and robustly increased with reperfusion time. This was associated with heavier compromise of blood vessel integrity, which was proven in the greater loss of tight junction protein ZO-1 after 2 hours of ischaemia in Ins2^{Akita/+} mice. These together with increased MMP-2 and MMP-9 expressions result in a more weakened blood vessel integrity and haemorrhagic transformation, which may account for further exacerbations and even the earlier death in Ins2^{Akita/+} mice.

Besides the presence of haemorrhage, significant increase of inflammatory responses also worsened the outcomes in Ins2^{Akita/+} mice. There was significant increase in p-Erk and p-p38 MAPK expressions only in Ins2^{Akita/+}, and the increase persisted at high levels at 22 hours after reperfusion. This suggested long-term exposure of hyperglycaemia results in earlier and more robust Erk1/2 and p38 MARK activation, and thereby triggering inflammatory response and neuronal cell death.

The increase in CHOP expression shortly after 2 hours of reperfusion following 2 hours of ischaemia in both Ins2^{+/+} and Ins2^{Akita/+} mice may associate with apoptosis. The more profound up-regulation of CHOP in Ins2^{Akita/+} mice may indicate additional apoptosis in the penumbra and infarct core under hyperglycaemia. CHOP up-regulation diminished at 22 hours after reperfusion, implying an early role of CHOP ischaemic stroke.

Most importantly, lutein treatment to Ins2^{Akita/+} mice in the 2hI/2hR group resulted in a lower mortality. Moreover, in the 0.5hI/23.5hR group with milder neurological deficits, lutein was able to reduce neurological scores, suggesting a neuroprotective effect to the penumbra, likely via its anti-inflammatory and anti-oxidative property that counteracting damages from inflammation, free radical, and reactive oxidative species generated after ischaemia/reperfusion injury.

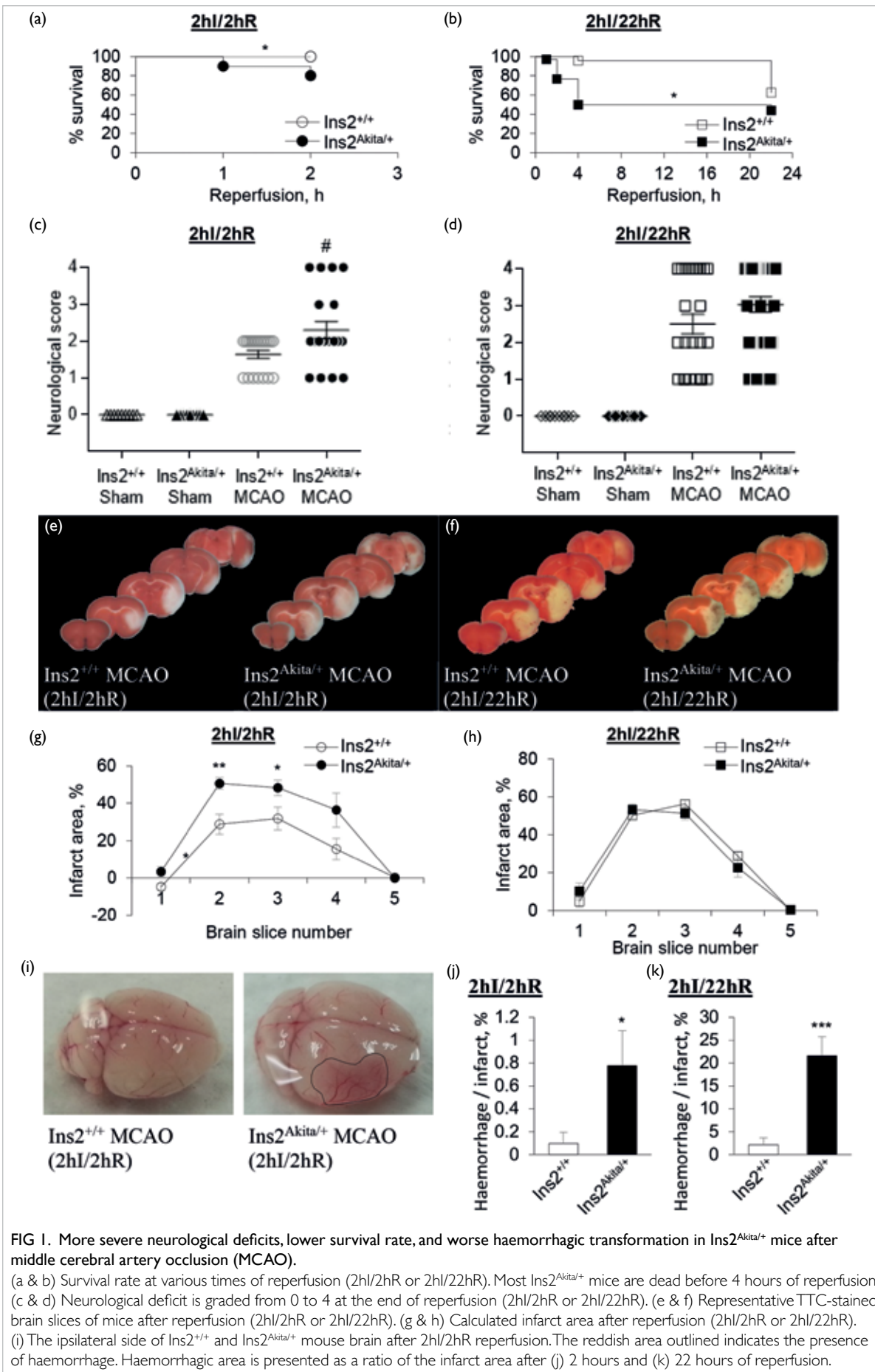


FIG 1. More severe neurological deficits, lower survival rate, and worse haemorrhagic transformation in Ins2^{Akita/+} mice after middle cerebral artery occlusion (MCAO). (a & b) Survival rate at various times of reperfusion (2hI/2hR or 2hI/22hR). Most Ins2^{Akita/+} mice are dead before 4 hours of reperfusion. (c & d) Neurological deficit is graded from 0 to 4 at the end of reperfusion (2hI/2hR or 2hI/22hR). (e & f) Representative TTC-stained brain slices of mice after reperfusion (2hI/2hR or 2hI/22hR). (g & h) Calculated infarct area after reperfusion (2hI/2hR or 2hI/22hR). (i) The ipsilateral side of Ins2^{+/+} and Ins2^{Akita/+} mouse brain after 2hI/2hR reperfusion. The reddish area outlined indicates the presence of haemorrhage. Haemorrhagic area is presented as a ratio of the infarct area after (j) 2 hours and (k) 22 hours of reperfusion.

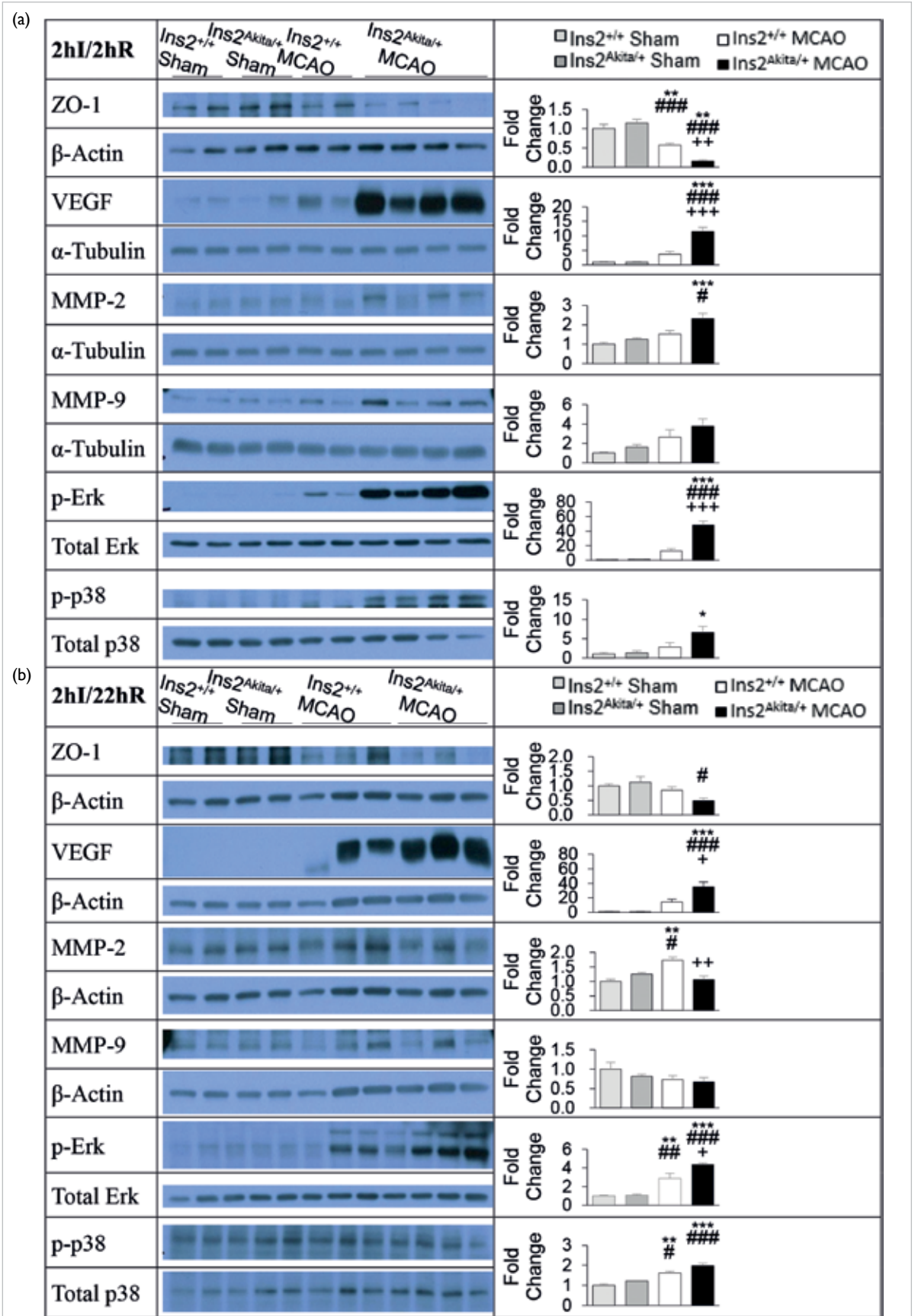
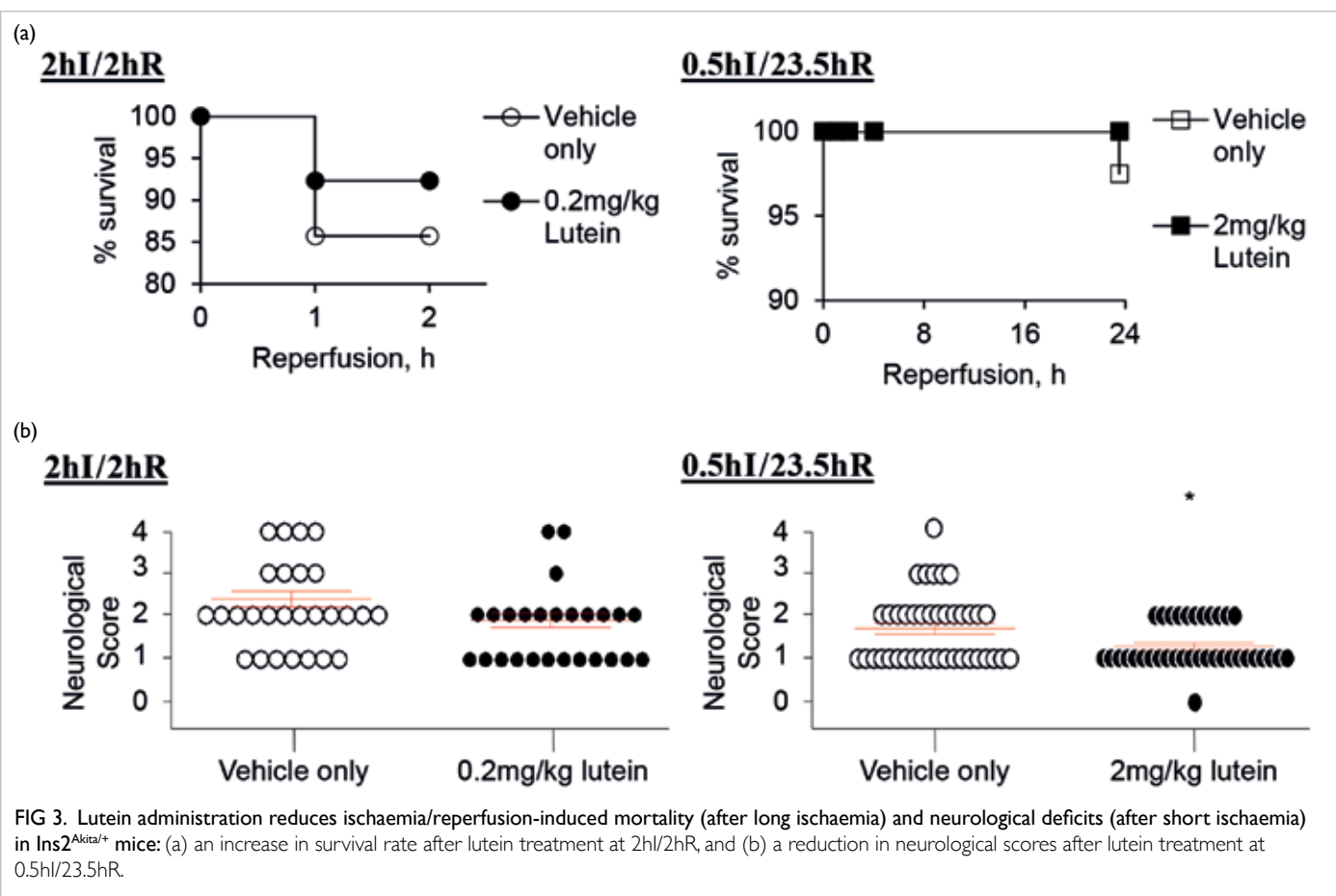


FIG 2. Vulnerable blood vessel integrity and increased inflammatory response in *Ins2^{Akit+/+}* mice at 2 hours after reperfusion: protein expressions of ZO-1 (a tight junction protein), VEGF, MMP-2, MMP-9, p-Erk, and p-p38 MAPK at (a) 2hI/2hR and (b) 2hI/22hR in *Ins2^{+/+}* and *Ins2^{Akit+/+}* mice. Protein expressions are semi-quantified using Western blot analysis; corresponding fold changes are shown in the right panel.



Conclusion

Hyperglycaemia plays an important role in the rapid exacerbation of stroke. After 2 hours of ischaemia, blood vessel integrity was compromised along with the presence of haemorrhagic transformation, extensive inflammation, and high mortality in diabetic mice at as early as 2 hours after reperfusion. We postulate these exacerbations are partially contributed by VEGF up-regulation, which has deleterious effects via triggering robust inflammation and vascular hyper-permeability. After 0.5 hour of ischaemia, hyperglycaemic *Ins2^{Akita/+}* mice displayed a delayed yet still significant development of infarct. Most importantly, lutein treatment was able to lower mortality (after long ischaemia) and neurological deficits (after short ischaemia). Lutein is therefore a potential treatment for stroke patients with type 1 diabetes.

Funding

This study was supported by the Health and Medical Research Fund, Food and Health Bureau, Hong Kong SAR Government (#03142256). The full report is available from the Health and Medical Research Fund website (<https://rfs1.fhb.gov.hk/index.html>).

References

1. Laing SP, Swerdlow AJ, Carpenter LM, et al. Mortality from cerebrovascular disease in a cohort of 23 000 patients with insulin-treated diabetes. *Stroke* 2003;34:418-21.
2. Secrest AM, Prince CT, Costacou T, Miller RG, Orchard TJ. Predictors of survival after incident stroke in type 1 diabetes. *Diab Vasc Dis Res* 2013;10:3-10.
3. Wang J, Takeuchi T, Tanaka S, et al. A mutation in the insulin 2 gene induces diabetes with severe pancreatic beta-cell dysfunction in the Mody mouse. *J Clin Invest* 1999;103:27-37.
4. Li SY, Yang D, Fu ZJ, Woo T, Wong D, Lo AC. Lutein enhances survival and reduces neuronal damage in a mouse model of ischemic stroke. *Neurobiol Dis* 2012;45:624-32.

Intracranial artery calcification to screen patients at high risk of recurrent stroke: abridged secondary publication

KS Wong *, XY Chen, TWH Leung, YW Siu, L Xiong, X Leng

KEY MESSAGES

1. Our study failed to validate the association between intracranial artery calcification (IAC) and recurrent stroke, likely owing to relatively short follow-up of 1 year. We will continue to follow up these patients to record the occurrence of ischaemic stroke and other vascular events.
2. The association between IAC and pulsatility index reflects that calcification within the arterial wall may cause arterial stiffness in cerebral arteries.

Hong Kong Med J 2020;26(Suppl 7):S42-4

HMRF project number: 11120161

¹ KS Wong, ¹ XY Chen, ¹ TWH Leung, ² YW Siu, ¹ L Xiong, ¹ X Leng

¹ Department of Medicine and Therapeutics, Prince of Wales Hospital, The Chinese University of Hong Kong

² Department of Diagnostic and Interventional Radiology, Kwong Wah Hospital

* Principal applicant and corresponding author: ks-wong@cuhk.edu.hk

Introduction

Intracranial atherosclerosis is a common cause of stroke, especially in Asian populations.¹⁻³ Arterial calcification is an active process of atherosclerosis. Computed tomography (CT) can be used to evaluate intracranial artery calcification (IAC) non-invasively. Evidence suggests associations between IAC and ischaemic stroke, vascular dementia, and other brain diseases. Our pilot study detected a high prevalence of IAC in Chinese and the association of IAC with age, history of ischaemic stroke, and white blood cell count.⁴ A case-control study suggested that IAC may be a risk factor of ischaemic stroke.⁵ Therefore, we aim to determine the predictive value of IAC on ischaemic stroke and its underlying mechanisms in a Chinese population using transcranial CT.

Methods

Consecutive patients were recruited from the acute stroke unit in Prince of Wales Hospital. Inclusion criteria were age of 40-85 years, Chinese ethnicity, diagnosed with ischaemic stroke according to World Health Organization stroke diagnostic criteria, presence of good temporal window, written informed consent given, and routine plain CT brain performed.

CT was performed using a 16-slice multi-detector row CT system (Light speed 16 plus, General Electric, Milwaukee [WI], USA). The unenhanced brain CT scans were acquired in axial mode with tilting along the occipito-meatal line, covering the base of the skull to vertex region and with parameters of 140 kVp, 170 mAs, and 2 s per rotation. Axial images were reconstructed at 0.625-mm intervals and stored as digital imaging and

communication in medicine data for analysis.

Calcification was defined as hyperdense foci with attenuation number ≥ 130 HU. Both qualitative and quantitative IAC properties were measured. Intracranial arteries were assessed, including the intracranial internal carotid artery, anterior cerebral artery, middle cerebral artery, posterior cerebral artery, basilar artery, and bilateral intracranial vertebral arteries. The extent and thickness of arterial calcification were scored on a five-point scale, using the 0.625 mm unenhanced axial CT images at bone window setting (window level, 300 HU; window width, 1500 HU).

Agatston score, volume score, and mean density were assessed quantitatively using a custom-made programme to MATLAB. Calcification segmentation was the most important step. All CT images were first reconstructed to three-dimensional (3D) images, and then transferred to 3D software (Analyze 12.0), by which IAC was segmented using the 'seeding method' (Fig). The source images and segmentations were transferred to ITK-SNAP software, which automatically generated the volume and mean density data of the outlined regions. For Agatston score assessment, the 3D images with IAC segments were reconstructed into 3-mm-thick-slice images by MATLAB, and the Agatston score was generated with an algorithm, in which a weighted value was assigned to the highest artery calcium density within the slice on each 3-mm-thick CT slice, with a weighted value of 1 for 130-199 HU, 2 for 200-299 HU, 3 for 300-399 HU, and 4 for ≥ 400 HU. This weighted value was then multiplied by the area of calcification in the same slice.

Patients were followed up for 1 year at outpatient clinics for stroke recurrence and

treatment. All cardiovascular events (myocardial infarction, cerebrovascular events) and death secondary to vascular disease were recorded. Regular follow-up was performed to record stroke recurrence until July 2016.

Results

Of 340 patients recruited, 331 underwent transcranial CT. IAC was identified in around 88.2% of patients. Median IAC volume was 64.9 (range, 12.2-272.4) mm³ and median total Agatston score was 24.0 (range, 2.8-118.5) [Table 1]. Recurrent stroke was recorded in 19 (5.7%) patients and myocardial infarction in 4 (1.2%) patients. The small sample size and low prevalence of recurrent stroke failed to determine any predictor.

Correlation between IAC and cerebral haemodynamic parameters in 318 (96.1%) patients was analysed. Both IAC Agatston score and IAC volume score were correlated with both high velocity (>140 cm/s) and high pulsatility index (>1.2) in the middle cerebral artery (all P<0.001) as well as in the vertebral-basilar artery (all P<0.001) [Table 2].

Discussion

Our findings failed to verify IAC as a predictor of recurrent stroke, partly owing to the low occurrence rate of recurrent stroke among our patients with mild to moderate stroke severity and the short follow-up of 1 year. Quantitative measurements of IAC (IAC Agatston score and IAC volume score) were found to be correlated with high systolic blood flow velocity and increased pulsatility index in intracranial cerebral arteries, indicating that IAC

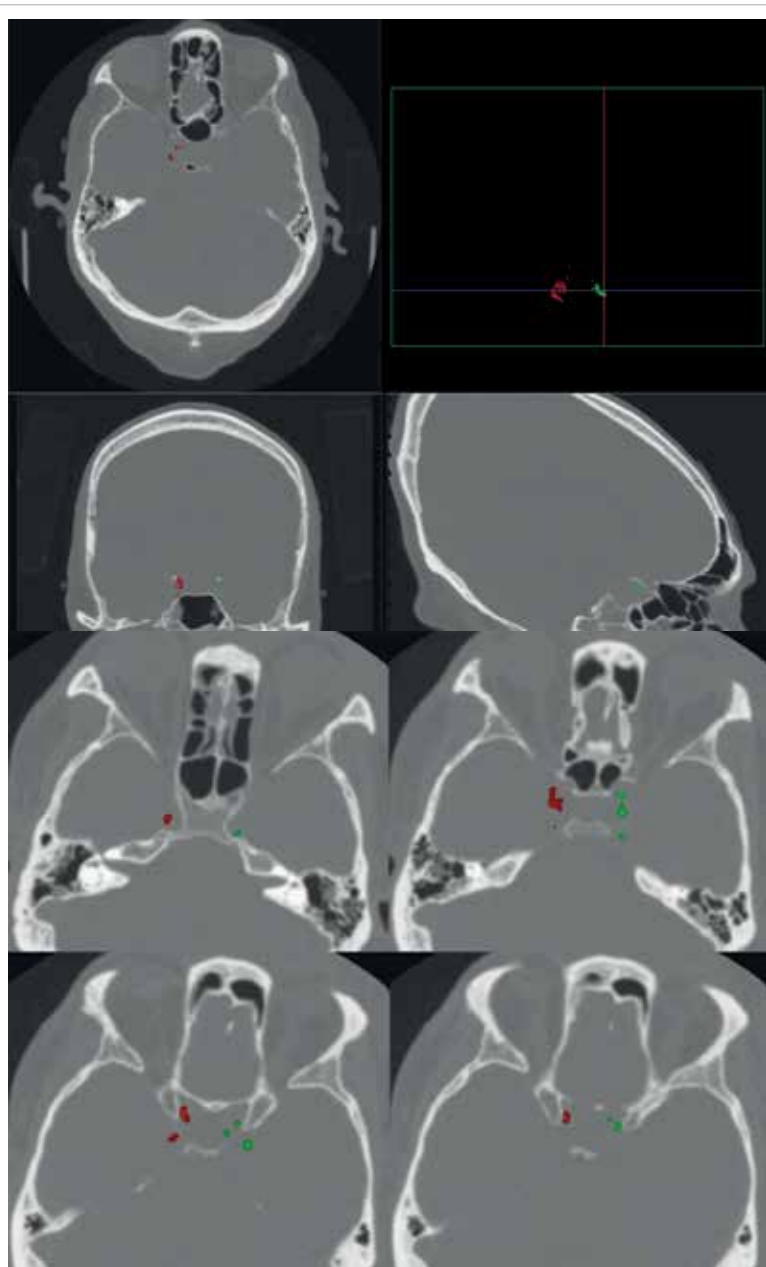


FIG. Semi-automatic segmentations of bilateral intracranial carotid artery calcification.

TABLE 1. Baseline characteristics of patients

Variable	Total (n=331)*
Age, y	65.3±12.0
No. of men	263 (79.5)
Hypertension	191 (57.7)
Diabetes mellitus	92 (27.8)
Chronic renal failure	12 (3.6)
Ischaemic heart disease	31 (9.4)
Ischaemic stroke history	52 (15.7)
Current smoker	79 (23.9)
Hyperlipidaemia	182 (55.0)
Presence of intracranial arterial calcification	292 (88.2)
Total intracranial arterial calcification volume, mm ³	64.9 (12.2-272.4)
Total Agatston score	24.0 (2.8-118.5)

* Data are presented as mean±standard deviation, No. (%) of cases, or median (interquartile range)

may cause generalised arterial stiffness within the cerebrovasculature.

There was selection bias in recruiting stroke patients because of poor temporal window in some female patients. This resulted in male predominance of participants. The requirements of written consent forms excluded patients with relatively severe stroke, especially those with movement disorders in upper limbs. Follow-up at 1 year was relatively short to investigate the effects of IAC on ischaemic stroke. We will continue to follow up these patients to record the occurrence of ischaemic stroke and other vascular events.

TABLE 2. Spearman correlation coefficients between cerebral haemodynamic parameters and intracranial arterial calcification (IAC) scores

	Overall (n=318)	IAC Agatston score		IAC volume score	
		Correlation coefficient	P value	Correlation coefficient	P value
Middle cerebral artery					
High velocity (>140 cm/s)	67 (21.1%)	0.228	<0.001	0.217	<0.001
High pulsatility index (>1.2)	121 (38.1%)	0.307	<0.001	0.318	<0.001
Vertebral-basilar artery					
High velocity (>100 cm/s)	23 (7.2%)	0.198	<0.001	0.194	<0.001
High pulsatility index (>1.2)	136 (42.8%)	0.407	<0.001	0.411	<0.001

Funding

This study was supported by the Health and Medical Research Fund, Food and Health Bureau, Hong Kong SAR Government (#11120161). The full report is available from the Health and Medical Research Fund website (<https://rfs1.fhb.gov.hk/index.html>).

Disclosure

The results of this research have been previously published in:

1. Wu XH, Chen XY, Wang LJ, Wong KS. Intracranial artery calcification and its clinical significance. *J Clin Neurol* 2016;12:253-61.
2. Wu X, Wang L, Zhong J, et al. Impact of intracranial artery calcification on cerebral hemodynamic changes. *Neuroradiology* 2018;60:357-63.
3. Wu XH, Chen XY, Fan YH, Leung TW, Wong KS. High extent of intracranial carotid artery calcification

is associated with downstream microemboli in stroke patients. *J Stroke Cerebrovasc Dis* 2017;26:442-7.

References

1. Wong KS, Li H, Lam WW, Chan YL, Kay R. Progression of middle cerebral artery occlusive disease and its relationship with further vascular events after stroke. *Stroke* 2002;33:532-6.
2. Wong KS, Huang YN, Gao S, Lam WW, Chan YL, Kay R. Intracranial stenosis in Chinese patients with acute stroke. *Neurology* 1998;50:812-3.
3. Wong KS, Li H, Chan YL, et al. Use of transcranial Doppler ultrasound to predict outcome in patients with intracranial large-artery occlusive disease. *Stroke* 2000;31:2641-7.
4. Chen XY, Lam WW, Ng HK, Fan YH, Wong KS. The frequency and determinants of calcification in intracranial arteries in Chinese patients who underwent computed tomography examinations. *Cerebrovasc Dis* 2006;21:91-7.
5. Chen XY, Lam WW, Ng HK, Fan YH, Wong KS. Intracranial artery calcification: a newly identified risk factor of ischemic stroke. *J Neuroimaging* 2007;17:300-3.

Gastrodia-Uncaria water extract and tissue plasminogen activator for treating embolus-induced cerebral ischaemia: abridged secondary publication

JW Xian, AYT Choi, WN Leung, L Li, CBS Lau, TWH Leung, CW Chan *

KEY MESSAGES

1. The treatment potential of Gastrodia-Uncaria water extract on cerebral ischaemia was demonstrated in terms of reduction of brain infarct volume of the brain, improvement of the motor behaviour recovery, stimulation of anti-oxidative enzyme, inhibition of matrix metalloproteinase, induction of neurotrophins, and maintenance of brain tissue integrity.
2. Intravascular administration of tissue plasminogen activator is well tolerated with oral administration of Gastrodia-Uncaria water extract, which may reduce the risk of tissue

plasminogen activator-induced intracranial haemorrhage.

Hong Kong Med J 2020;26(Suppl 7):S45-7

HMRF project number: 11120381

¹ JW Xian, ¹ AYT Choi, ¹ WN Leung, ² L Li, ¹ CBS Lau, ³ TWH Leung, ¹ CW Chan

¹ School of Chinese Medicine, The Chinese University of Hong Kong

² Department of Chemistry, University of Alberta

³ Department of Medicine and Therapeutics, The Chinese University of Hong Kong

* Principal applicant and corresponding author: francischan.2010@gmail.com

Introduction

Stroke is the third cause of death worldwide and leads to disability. The recombinant tissue plasminogen activator (tPA) is the only approved drug to treat acute ischaemic stroke. However, it has a narrow treatment window and increases the risk of haemorrhagic transformation. Neuroprotection is thus explored to reduce brain injury. The 11-herb Gastrodia-Uncaria decoction is a commonly prescribed Chinese herbal medicine for stroke. Gastrodia Rhizome and Uncaria Ramulus are the two main components in the decoction. They may act synergistically in protecting neurons from oxygen glucose deprivation/reperfusion through inhibiting oxidative stress and apoptosis.¹ We aimed to study the neuroprotective effect of Gastrodia-Uncaria water extract (GUW) with or without tPA post-onset of ischaemia. The efficacy of GUW plus tPA versus tPA alone and GUW alone on cerebral ischaemia and their drug interaction were also investigated.

Methods

A rat model of embolic-induced middle cerebral artery occlusion was used. Neurological deficits, behavioural rearing, and brain infarct volume were tested for the effect of GUW. The efficacy of GUW and tPA and their drug interaction were evaluated using *in vivo* molecular imaging, histology, immunohistochemistry, and gene expression.

Results

The use of GUW post-stroke significantly reduced brain infarct volume and improved motor behaviour recovery. It enhanced efficacy of tPA against embolic-induced cerebral ischaemia and suppressed tPA-induced matrix metalloproteinases (MMP) activity. After middle cerebral artery occlusion, GUW increased superoxide dismutase activity but tPA did not. GUW upregulated gene expression of neutrophins and overcame downregulation induced by tPA.

When GUW was applied after stroke, similar results were demonstrated. GUW showed neuroprotective potential against cerebral ischaemia in terms of brain tissue integrity, reduction of infarct volume, suppression of MMP activity, and enhancement of the motor behaviour recovery. GUW stimulated both catalase and superoxide dismutase activities. The use of both GUW and tPA increased the activity of catalase, superoxide dismutase, and GPx. GUW upregulated gene expression of some neutrophins (BDNF, GDNF, and NGF). It also increased BDNF and GDNF expression when tPA was applied.

Discussion

Stroke is a leading cause of death and disability worldwide. Its treatment and research are challenging because of its clinical variability in terms of duration, localisation, and severity of

ischaemia, as well as patient age and comorbid systemic diseases.² Oxidative stress is a major cause leading to brain damage and a potential contributor to the pathophysiological consequences following cerebral ischaemic stroke. Oxidative stress leads to oedema and destructs the blood-brain barrier (BBB). Reactive oxygen species triggers oxidative damage of lipids and proteins, leading to excitotoxic stimulation during reperfusion of ischaemic tissue. Furthermore, excessive free-radical production increases the risk of BBB disruption, which may contribute to more serious consequences such as brain oedema. Under normal conditions, the anti-oxidative enzymes including superoxide dismutase, catalase, glutathione, glutathione reductase/glutathione peroxidases (GR/GPX) are up-regulated to reduce harmful effects of oxidative stress parenchyma. However, tPA may suppress antioxidant (eg, vitamins) or free-radical scavengers (eg, edaravone) and result in more damage in brain parenchyma.

Gastrodia elata and its active ingredients exhibit anti-oxidative effect against focal cerebral ischaemia. Gastrodin is a major compound to protect against cerebral ischaemia by improving anti-oxidant and anti-inflammation activities. In our previous study, GUV treatment was found to upregulate the anti-oxidative pathway against oxygen-glucose deprivation-induced injury on PC12 cells in a rat model of middle cerebral artery occlusion.¹ Nonetheless, the changes in metabolite profiles of GUV and even *Gastrodia elata* during the neuroprotective events are not known. The use of GUV post-stroke increased the activity of anti-oxidative enzyme significantly. Furthermore, malondialdehyde concentration was reduced in GUV groups. This implies that GUV enhances the antioxidant mechanism to protect the cerebral ischaemia rats from reactive oxygen species-induced oxidative damage.

During cerebral ischaemia, MMP activities were increased. MMPs disrupt BBB integrity via digestion of endothelial basal lamina. Both MMP-2 and MMP-9 mainly participate in ischaemic damage processes. They are further activated by the reperfusion phase following cerebral ischaemia when blood clots are digested by endogenous or exogenous tPA. The BBB disruption may contribute to serious consequences such as brain oedema and intracerebral haemorrhage.

In our study, GUV inhibited the activity of MMPs and reduced BBB impairment. It rescued the neuronal cells from cell death and hence protected animal against ischaemic injury. The inhibitory effect of GUV on MMPs may repair the ischaemic brain, particularly during angiogenesis and reestablishment of cerebral blood flow. During cerebral ischaemia, reactive oxygen species and reactive nitrogen species are responsible for the

activation of MMP-9. The formation of nitrous oxide during ischaemia facilitates the activation of MMP-9 by S-nitrosylation. Based on the anti-oxidative, anti-nitrosative, and anti-inflammatory effect of *Gastrodia elata* and *Uncaria rhynchophylla*, GUV attenuated cerebral ischaemia/reperfusion injury might be partly via inhibition of MMP activities.

Intravascular administration of tPA is the only Food and Drug Administration approved medical therapy for cerebral ischaemia. However, tPA may penetrate through the permeabilised BBB and lyse the blood vessels in brain. Excess tPA activity also accumulates free radicals and increases MMP activities, leading to neuronal damage, mainly involving inflammation and oxidative stress pathway. Nonetheless, inadequate application of tPA leads to life-threatening brain oedema and haemorrhage in patients during the reperfusion phase.³ The haemorrhage may associate with thrombin activation of MMP-9 in astrocytes through protease-activated receptor 1. There are no available medications providing neuroprotective effect to neurons in the reperfusion phase to treat such cerebral oedema and haemorrhage.

In our study, the MMPs expression was significantly increased in the reperfusion phase after tPA administration. However, GUV suppressed tPA-induced MMP activities in this reperfusion phase. This suggests that the treatment of GUV might maintain BBB integrity through down-regulation of MMP activities that involve inflammation after cerebral ischaemia onset. Collectively, GUV significantly reduced the MMP activities in the brains of rats. The integrated therapy of tPA with GUV can provide protection in both ischaemic and reperfusion phase and reduce the risk of haemorrhage.

Neurotrophins are a family of growth factor proteins including BDNF, NGF, and GDNF. They are important in neuronal development and function and are therapeutic options for brain injury. NGF has demonstrated neuroprotection following neonatal rat hypoxia-ischaemia. GDNF has shown to have neuroprotective effects following ischaemic brain injury when introduced to the brain by viral vectors or GDNF-expressing cells. BDNF is a promising therapeutic candidate.⁴ These growth factors potentially prevent cell death and stimulate neuronal function.⁵ Our results showed that GUV increased the neurotrophins' gene expression that provided neuroprotection effect against ischaemic damage.

Together with the anti-oxidant, anti-MMP, and enhancing neurotrophin effect, GUV treatment reduced brain infarct volume. Histological results showed an increase in tissue integrity in the ischaemic region. Thus, rats subjected to GUV treatment showed improvements in neurological deficit score.

Conclusion

GUW has treatment potential on cerebral ischaemia. Intravascular administration of tPA is well tolerated with oral administration of Gastrodia-Uncaria water extract, which reduces the risk of tPA-induced intracranial haemorrhage.

Funding

This study was supported by the Health and Medical Research Fund, Food and Health Bureau, Hong Kong SAR Government (#11120381). The full report is available from the Health and Medical Research Fund website (<https://rfs1.fhb.gov.hk/index.html>).

Disclosure

The results of this research have been previously published in:

1. Xian JW, Choi AY, Lau CB, Leung WN, Ng CE, Chan CW. Gastrodia and Uncaria (tianma gouteng) water extract exerts antioxidative and antiapoptotic effects against cerebral ischemia in vitro and in vivo.

Chin Med 2016;11:27.

2. Huan T, Xian JW, Leung WN, Li L, Chan CW. Cerebrospinal fluid metabolomics after natural product treatment in an experimental model of cerebral ischemia. OMICS 2016;20:670-80.

References

1. Xian JW, Choi AY, Lau CB, Leung WN, Ng CE, Chan CW. Gastrodia and Uncaria (tianma gouteng) water extract exerts antioxidative and antiapoptotic effects against cerebral ischemia in vitro and in vivo. Chin Med 2016;11:27.
2. Moskowitz MA, Lo EH, Iadecola C. The science of stroke: mechanisms in search of treatments. Neuron 2010;67:181-98.
3. Zhang Y, Wang Y, Zuo Z, et al. Effects of tissue plasminogen activator timing on blood-brain barrier permeability and hemorrhagic transformation in rats with transient ischemic stroke. J Neurol Sci 2014;347:148-54.
4. Larphaveesarp A, Ferriero DM, Gonzalez FF. Growth factors for the treatment of ischemic brain injury (growth factor treatment). Brain Sci 2015;5:165-77.
5. Nagahara AH, Tuszynski MH. Potential therapeutic uses of BDNF in neurological and psychiatric disorders. Nat Rev Drug Discov 2011;10:209-19.

AUTHOR INDEX

Baum L	17, 20	Leng X	42
Bunting M	29	Leung TWH	42, 45
Chan AML	20	Leung WN	45
Chan CW	45	Li AM	7
Chan KH	29	Li L	45
Chan TF	4	Li M	33
Chan WC	13	Lin ZX	20
Chang RCC	20, 26	Lo ACY	37
Chen XY	42	Lo FMI	4
Cheng JCY	10	Ma SL	13
Choi AYT	45	Malampati S	33
Chow AHL	17	McManus A	7
Choy RKW	10	Mok VCT	23
Chung SK	29, 33, 37	Moreau A	10
Dow B	13	Ng DTC	37
Durairajan SSK	33	Ng KM	26
Esteban JA	20	Ng RCL	29
Fung FKC	37	Pautler RG	17
Fung LWE	4	Shah A	26
Han QB	33	Siu YW	42
Hau WLE	4	Sreenivasmurthy SG	33
Ho YS	26	Sung RYT	7
Iyaswamy A	33	Tam BKC	37
Jian M	29	Tsui SKW	4
Kammala AK	33	Wang M	26
Ke Y	23	Wang YX	17
Kwok SLJ	4	Wong KS	42
Lai AKW	37	Wong YH	20
Lam LCW	13	Wu EX	17
Lam TP	10	Xian JW	45
Lau CBS	45	Xiong L	42
Lautenschlager N	13	Yip BHK	10
Lee WYW	10	Yung WH	20, 23
Legido-Quigley C	26		

Disclaimer

The reports contained in this publication are for reference only and should not be regarded as a substitute for professional advice. The Government shall not be liable for any loss or damage, howsoever caused, arising from any information contained in these reports. The Government shall not be liable for any inaccuracies, incompleteness, omissions, mistakes or errors in these reports, or for any loss or damage arising from information presented herein. The opinions, findings, conclusions and recommendations expressed in this publication are those of the authors of the reports, and do not necessarily reflect the views of the Government. Nothing herein shall affect the copyright and other intellectual property rights in the information and material contained in these reports. All intellectual property rights and any other rights, if any, in relation to the contents of these reports are hereby reserved. The material herein may be reproduced for personal use but may not be reproduced or distributed for commercial purposes or any other exploitation without the prior written consent of the Government. Nothing contained in these reports shall constitute any of the authors of these reports an employer, employee, servant, agent or partner of the Government.

Published by the Hong Kong Academy of Medicine Press for the Government of the Hong Kong Special Administrative Region. The opinions expressed in the *Hong Kong Medical Journal* and its supplements are those of the authors and do not reflect the official policies of the Hong Kong Academy of Medicine, the Hong Kong Medical Association, the institutions to which the authors are affiliated, or those of the publisher.